

KfK 3733

Mai 1984

Neutron Irradiation Effects on Superconducting and Stabilizing Materials for Fusion Magnets

W. Maurer

Institut für Technische Physik

Kernforschungszentrum Karlsruhe

KERNFORSCHUNGSZENTRUM KARLSRUHE

Institut für Technische Physik

KfK 3733

Neutron Irradiation Effects on Superconducting and
Stabilizing Materials for Fusion Magnets

W. Maurer

KERNFORSCHUNGSZENTRUM KARLSRUHE GMBH, KARLSRUHE

Als Manuskript vervielfältigt
Für diesen Bericht behalten wir uns alle Rechte vor

Kernforschungszentrum Karlsruhe GmbH
ISSN 0303-4003

Abstract

Available low-temperature neutron irradiation data for the superconductors NbTi and Nb₃Sn and the stabilization materials Cu and Al are collected and maximum tolerable doses for these materials are defined. A neutron flux in a reactor of about 10^9 n/cm² s at the magnet position is expected. However, in fusion experiments the flux can be higher by an order of magnitude or more. The energy spectrum is similar to a fission reactor. A fluence of about 10^{18} n/cm² results during the lifetime of a fusion magnet (about 20 full power years). At this fluence and energy spectrum no severe degradation of the superconducting properties of NbTi and Nb₃Sn will occur. But the radiation-induced resistivity is for Cu about a twentieth of the room temperature resistivity and a tenth for Al.

Neutronenbestrahlungseffekte in Supraleiter- und Stabilisierungsmaterialien für Fusionsmagnete

Zusammenfassung

Verfügbare Tieftemperaturbestrahlungsdaten für die Supraleiter NbTi und Nb₃Sn und die Stabilisierungsmaterialien Cu und Al sind gesammelt worden, und maximal tolerierbare Dosen für diese Materialien werden definiert. Am Magneten eines Fusionsreaktors wird ein Neutronenfluß von 10^9 n/cm² s erwartet. In Fusionsexperimenten kann der Fluß jedoch um eine Größenordnung oder mehr höher sein. Das Energiespektrum ist ähnlich dem eines Spaltungsreaktors. Während der Lebensdauer eines Fusionsmagneten (ungefähr 20 Volleistungsjahre) resultiert daraus eine Fluenz von ungefähr 10^{18} n/cm². Bei dieser Fluenz und diesem Energiespektrum treten keine schweren Degradationen der supraleitenden Eigenschaften von NbTi und Nb₃Sn auf. Jedoch ist der strahlungsinduzierte Widerstand für Cu ungefähr ein Zwanzigstel des Raumtemperaturwiderstandes und ein Zehntel für Al.

Table of Contents

	Page
1. Introduction	1
2. Working Conditions of Superconducting Magnets in a Fusion Reactor	2
3. Neutron Irradiation Effects on NbTi and Nb ₃ Sn	8
3.1 General	8
3.2 Neutron Irradiation of NbTi	8
3.3 Neutron Irradiation of Nb ₃ Sn	11
3.4 Comparison of NbTi and Nb ₃ Sn	16
4. Neutron Irradiation Effects on Cu and Al	17
4.1 General	17
4.2 Neutron Irradiation Effects on Cu and Al	18
4.2.1 Radiation-Induced Resistivity in Cu and Al	18
4.2.2 Saturation Behaviour of the Defect Resistivity for Cu and Al	31
4.2.3 Annealing Behaviour	33
4.2.4 Magnetoresistance	35
4.2.5 Mechanical Properties	42
4.2.6 Conclusions	45
5. Composite Superconductors	46
References	50

1. Introduction

The aim of this report is to collect available low-temperature neutron irradiation data for the superconductors NbTi and Nb₃Sn and the stabilizing materials and to define maximum tolerable doses for these materials.

Many experimental studies on the behaviour of NbTi and Nb₃Sn during particle irradiation were performed. Especially low temperature neutron irradiation is of interest for the use of superconducting magnets in fusion devices. Therefore, irradiation results with charged particles are only included in this report if necessary for comparison. Historically, irradiation with charged particles were of great interest for the application of superconducting magnets in accelerators /1, 2/. But with growing fusion activities neutron irradiations became more interesting.

Irradiation of superconductors changes the metallurgical structure and so the flux pinning behaviour. Radiation effects greatly depend upon initial metallurgical conditions of the sample to be irradiated. Many studies investigate the migration of radiation-induced defects, the formation of defect clusters and the annealing behaviour of the defects. The magnet designer depends more on the knowledge of "overall" properties of the superconductors, especially the transition temperature T_c , the upper critical magnetic field B_{c2} and the current carrying capacity J_c . Therefore, these data are collected when available.

Data for Cu and Al are needed for low temperatures because these materials are used as stabilizers in superconducting magnets, which are operated at temperatures of about 5 K, as well as for the temperature range of room temperature to about 500 K. These data are necessary to design normal conducting magnets which operate in a very high neutron flux. Such normal conducting magnets are considered either to be used in Tokamaks as passive coils for plasma control or as insert magnets in high field mirror coils to rise the mirror field into the range of above 20 T.

In general, irradiation influences considerably the resistivity of Cu and Al. The resistivity at low temperature is dominated by impurities and lattice imperfections. Irradiation particles generate new Frenkel pairs which change the scattering properties of conduction electrons. The mean free

path of the electrons is generally reduced and therefore the resistivity enhanced. This has a profound effect on the stabilization of superconducting magnets. However, at room temperature the resistivity change is dominated by transmutation products, because Frenkel pairs anneal nearly completely out.

2. Working Conditions of Superconducting Magnets in a Fusion Reactor

Superconducting magnets operate near liquid helium temperature. During cool-down large thermal stresses occur. Especially for high field magnet operation large electromagnetic Lorentz forces are acting. Large asymmetric forces resulting in twisting moments appear in time varying magnetic fields.

In fusion reactors neutron and γ -irradiation with high intensity and a broad energy spectrum influence the properties of superconducting materials, stabilizing materials, insulators, structural materials and deposit heat into the coolant medium helium. The low temperature, the stress and the radiation are synergic at the same time. In most irradiation experiments at low temperature no synergic effects are investigated because no magnetic field during irradiation is applied on the sample. For example, the magnetic field or applied stress during irradiation may influence the defect formation or migration and so the current carrying capacity of the superconductor.

A first wall loading of 1 MW/m^2 corresponds to a 14.1 MeV neutron flux of about $4.43 \times 10^{13} \text{ n cm}^{-2} \text{ s}^{-1}$. A fluence of $1.4 \times 10^{21} \text{ n/cm}^2$ (14.1 MeV neutron) produces 1 MWy/m^2 . Fluences in fusion reactors are much higher than the values where e. g. severe degradation of the superconducting properties begins. Therefore, the neutron flux through the first wall must be attenuated by a factor of about 10^{-6} to 10^{-8} (depending on the special design of the fusion device) to avoid a catastrophic degradation of the materials properties in the superconducting magnet.

Together with the attenuation of the neutron flux the neutron energy spectrum is changed during penetration of the blanket and shield.

McCracken and Blow /3/ calculated the flux values (see Fig. 2-1) and the neutron energy spectrum for a conceptual fusion reactor and compared it with an experimental spectrum used by Schilling et al. /4/ (see Fig. 2-2). The same comparison for the Kyoto University Research Reactor is shown in Fig. 2-3 and for the Research Reactor Garching in Fig. 2-4. The figures show that the expected neutron spectrum at the magnets is fairly well reproduced by fission reactors. It should be mentioned that approximately 20 % of the neutrons are expected to have energies greater than 1 MeV and about 5 % have energies greater than 4 MeV.

Although it is anticipated that the neutron spectrum at the magnet position will be somewhat softer than a fission spectrum with a small fraction of high-energy neutrons, regions, where the shielding is not as effective as the average, with higher fluxes of the higher-energy neutron component will occur ("hot spot"). This will influence the lifetime of magnet components. A quantitative knowledge of the radiation damage in the magnet materials is essential for the magnet designer. Therefore, three-dimensional calculations of damage rates in the magnet materials are necessary.

Abdou /7/ calculated the radiation levels and spectra at and within a special tokamak magnet system. His results show, that the neutron and gamma fluxes, the atomic displacements in Nb, Cu and Al and the radiation doses in typical insulators (Epoxy, Mylar) decrease by one order of magnitude over a depth of about 30 cm. Over the same length the hydrogen and helium production decrease by two orders of magnitudes.

Another criterion is the tolerable refrigeration power for the magnets. Choosing a value for the power deposit in the magnet in the order of some mW/cm^3 or less, the required attenuation factor is less than 10^{-6} . The exact limit has to be defined for an experimental device or a reactor by systems optimization. Designs for experimental devices consider values of about $10 \text{ mW}/\text{cm}^3$.

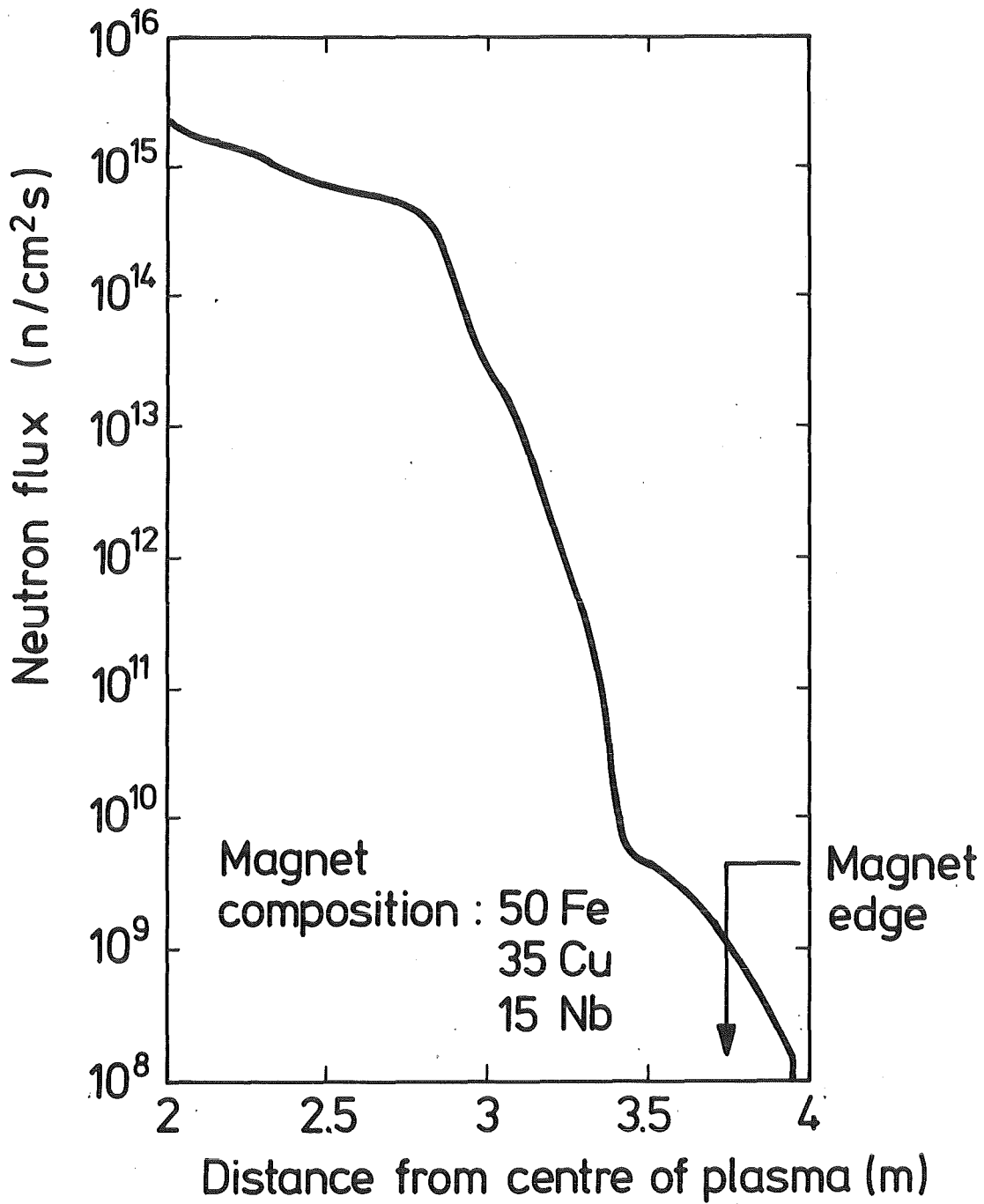


Fig. 2-1: Neutron flux in the blanket of a typical fusion reactor calculated using a Monte Carlo neutron code /3/. The magnet edge is at 375 cm. The total wall loading is 10 MWm⁻².

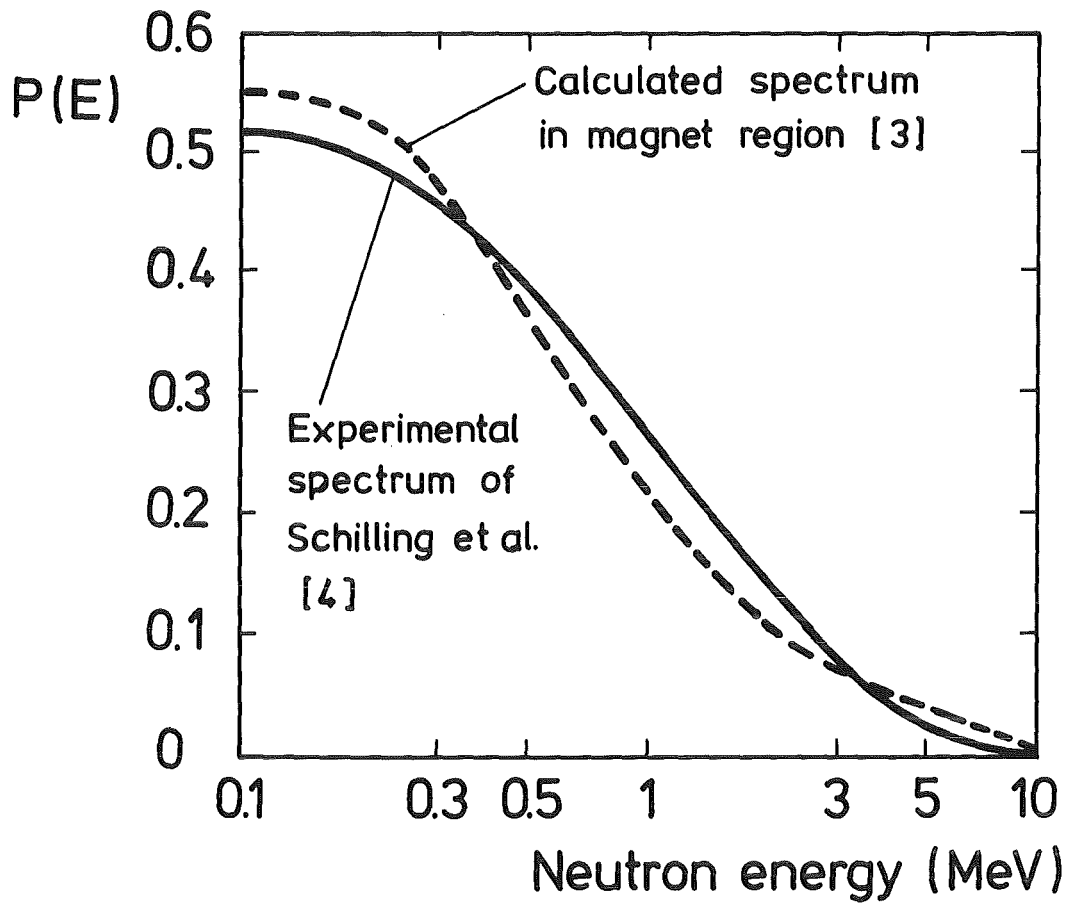


Fig. 2-2: Comparison of the neutron energy spectrum in the experimental irradiation facility at Jülich used by Schilling /4/ and calculated values /3/.

Definition:

$$P(E) = \frac{\int_0^{\infty} \phi(E') dE'}{\int_0^{\infty} \phi(E') dE'}$$

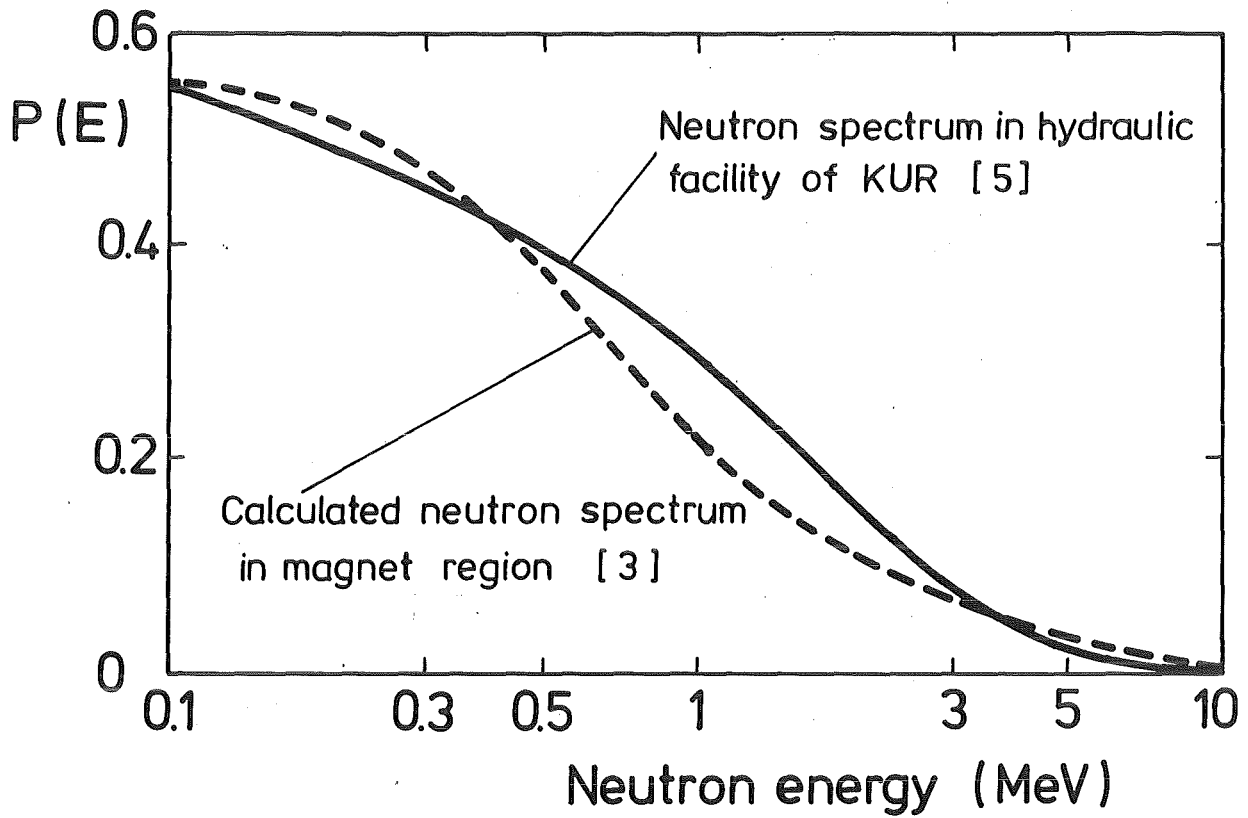


Fig. 2-3: Comparison of neutron energy spectrum in the Kyoto University Research Reactor /5/ and calculated values /3/.

P(E) is defined in Fig. 2-2.

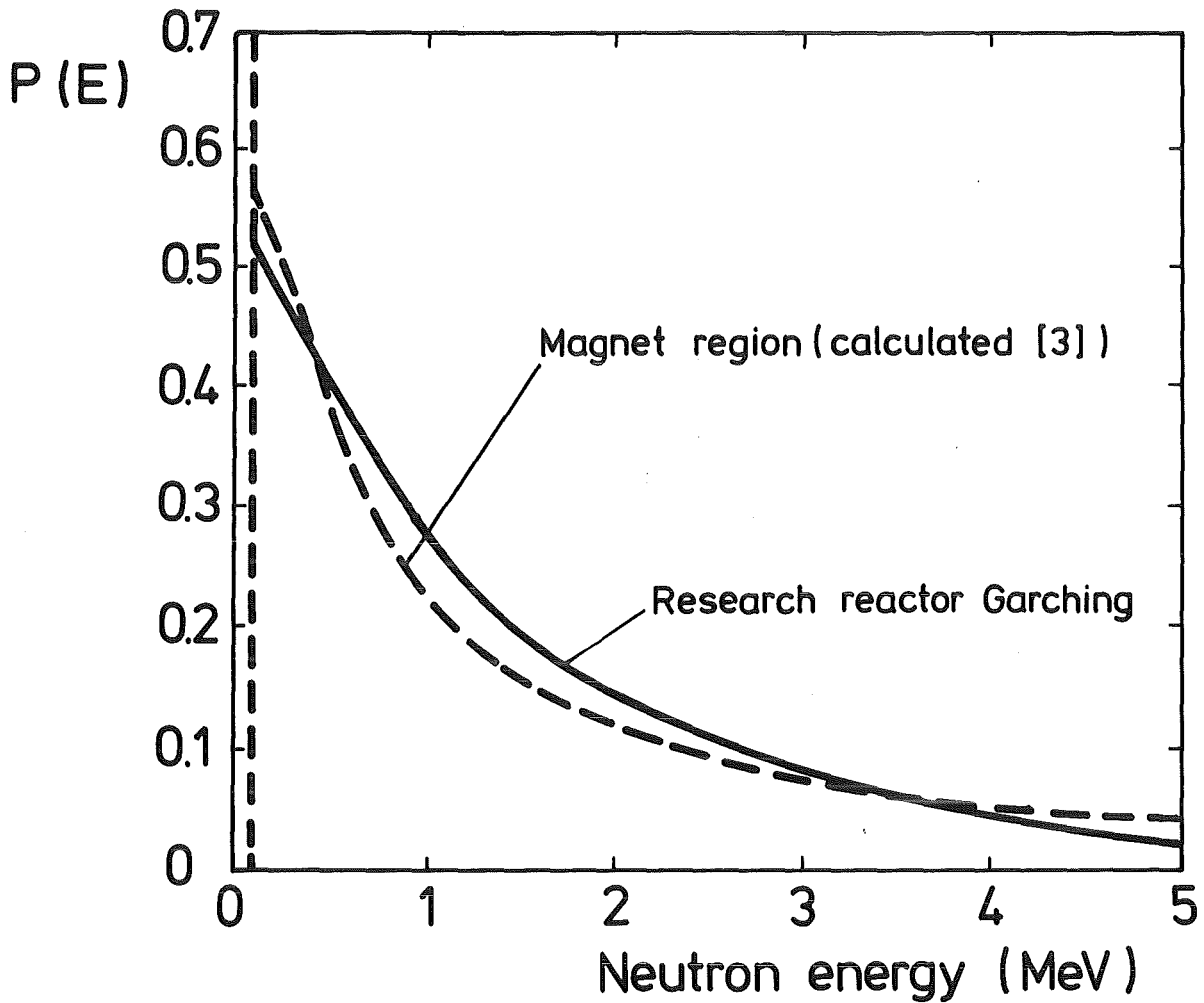


Fig. 2-4: Comparison of the neutron energy spectrum in the Research Reactor Garching used by Soell /e.g. 6/ and calculated values /3/.
P(E) is defined in Fig. 2-2.

3. Neutron Irradiation Effects on NbTi and Nb₃Sn

3.1 General

There are many reports on the irradiation behaviour of superconducting materials. Irradiation temperatures are ambient temperature, the temperature of 1N₂ 77 K and the temperature of liquid helium 4 K. Many materials were irradiated, e. g. Nb, Nb₃Sn, Nb₃Al, V₃Ga, V₃Si, Nb₃Al, NbZr, NbTi, ... NbTi and Nb₃Sn are particularly important for the magnet designer. So the references /3/ to /16/ review the radiation behaviour of either superconducting materials or superconducting magnets including the radiation behaviour of stabilizing and insulating materials. Beyond that, there are many papers where single aspects with respect to the radiation behaviour of materials or magnets are discussed, /17/ to /50/. The reports /28/ to /50/ discuss especially the irradiation effects on A15 superconductors. Report /50/ is a review on the neutron irradiation effects on superconducting compounds. This interest in A15 superconductors was because in the early seventies it was found that fluences of the order of 10^{19} n/cm² produce only up to 20 % reduction of the critical current of NbTi at 4 T. For Nb₃Sn, however, the same fluence reduced the critical current at 4 T by more than 95 %. These results suggest that the A15 high field superconductors are more sensitive to neutron irradiation relative to other types of superconductor alloys. But the irradiation temperature was about 60 °C, so the results were not representative for the low temperature behaviour.

3.2 Neutron Irradiation of NbTi

NbTi is used in most superconducting magnets with magnetic fields up to 8 T. This material is relatively inexpensive, mechanically stable and easily fabricated.

NbTi conductors are commercially available as multifilamentary conductors, i. e. a large number of NbTi filaments of diameters in the order of 10 μm embedded in a normal conducting metal, usually copper. Also single core conductors are available. But only the multifilamentary conductors are important for large magnet systems up to about 8 T.

The superconducting properties can be varied by various metallurgical treatments. But NbTi has relatively low values of J_c (B, T), T_c and B_{c2} as compared with Nb_3Sn . Fig. 3-1 shows the critical current - critical field - critical temperature diagram of a special NbTi superconductor /51/. The critical temperature is about 9 K and the upper critical magnetic field is about 10 T for 4.2 K.

Most of the neutron irradiation experiments were performed to establish criteria for the selection of conductors suited in an optimum way for applications involving neutron irradiation.

From the data reported about NbTi irradiation with fission reactor neutrons a fairly consistent picture of radiation-induced effects has emerged. For the magnet designer, the following conclusions are important:

- The decrease of the transition temperature T_c with neutron fluence is very small and may be neglected for application considerations. In /16, 26, 27/ a decrease of 0.15 K for fluences up to 9×10^{18} n/cm² (E > 1 MeV) is reported. The transition width (usually 1 K) remained unchanged.
- The change of the upper critical field B_{c2} is also expected to be very small. There are very few experiments and a more detailed investigation of radiation effects on B_{c2} would be desirable.
- NbTi conductors with relatively low initial current density show an enhancement of the current density after irradiation, while relatively high initial current densities decrease due to irradiation. Therefore, optimized commercial conductors always degrade after neutron irradiation. As a rule of thumb, a 10 % decrease of the current density occurs at a fluence of about $\phi \cdot t \sim 3 \times 10^{18}$ n/cm² (E > 0.1 MeV). The experimental results for the change in the critical current density of NbTi with neutron fluence up to 5×10^{18} n cm⁻² can be approximated /13/ as

$$J_c = J_{c0} \exp(-\alpha \cdot \phi \cdot t)$$

where J_{c0} is the critical current density before irradiation and $\alpha = 3.5 \times 10^{-20}$ cm⁻². The fluence $\phi \cdot t$ is an abbreviation for $\int_0^{t_{\max}} \phi dt$.

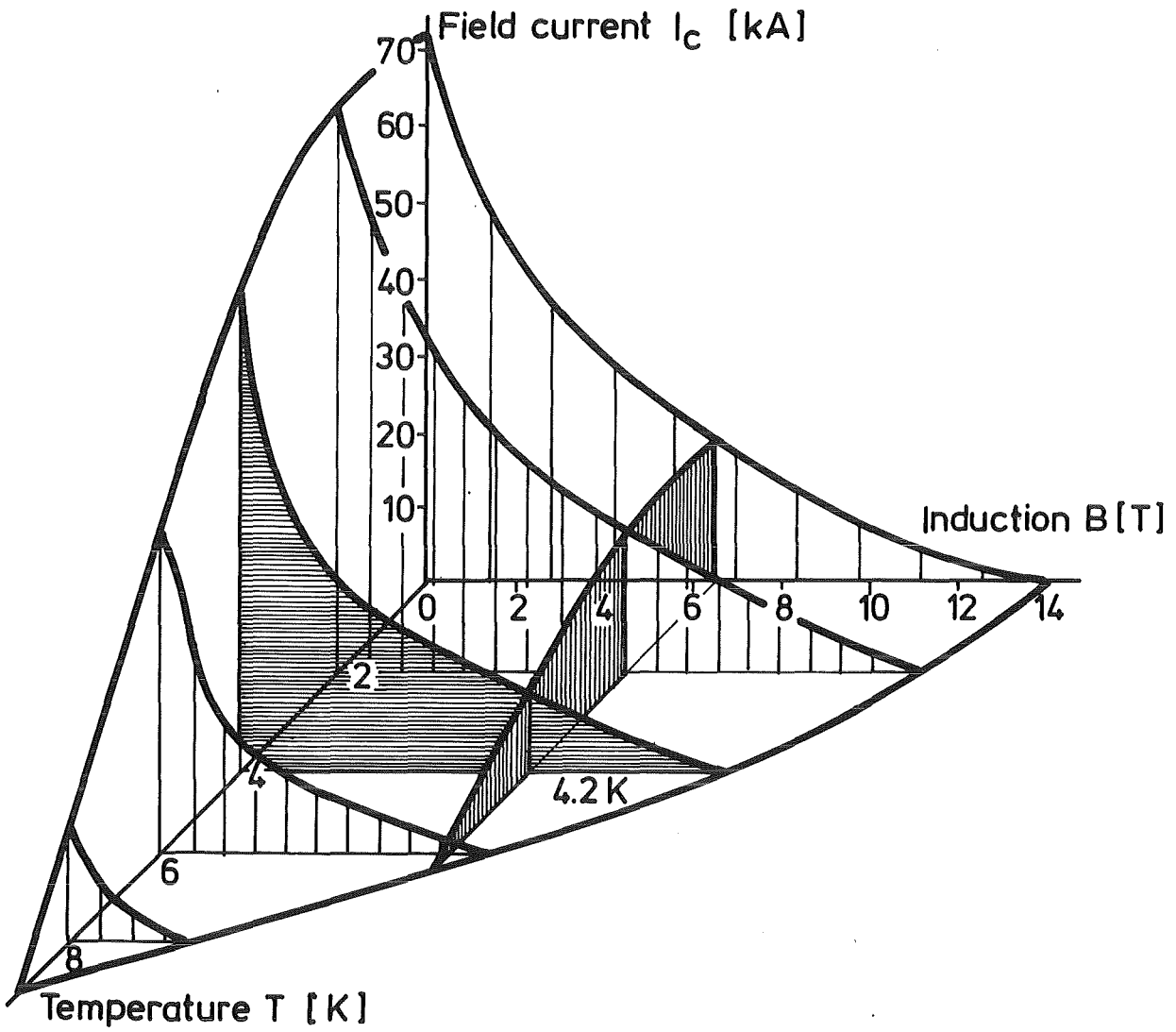


Fig. 3-1: I_c - B_c - T_c diagram of Niobium-Titanium superconductor /51/

The change of the critical current density can be explained consistently by assuming that the defects produced by irradiation affect the pinning strength of the dislocation cells.

- Annealing to room temperature and, in particular, multiple thermal cycles lead to almost complete recovery of J_c . This is consistent with the pinning mechanism based on the radiation-induced change of the normal state resistivity.
- Most of the work performed on reasonably high J_c superconductors shows that the changes of J_c are independent of magnetic fields up to about 6 T (0 - 6 T is usually investigated).

Irradiation experiments with high energy (14 MeV) "fusion neutrons" are scarce. Van Konynenburg, Guinan and Kinney /25/ irradiated NbTi wires with 14.8 MeV neutrons of the RTNS-II. They irradiated at 4.2 K up to a fluence of 8×10^{16} n/cm². Critical currents of NbTi were measured before and after irradiation in magnetic fields up to 10 T. The critical current decreased of about 3 % at 4 T and the transition temperature decreased of about 0.6 K. This is about a factor of 4 to 5 larger than observed for this level of damage in fission reactor fast neutron irradiations at 4.2 K. Within the precision of the measurement no changes were observed in the upper critical field or in the critical current at 6 T, 8 T and 10 T. In this high energy range, more experimental data are needed.

3.3 Neutron Irradiation of Nb₃Sn

The advantage of Nb₃Sn is the relatively high critical temperature of ~ 18 K and the upper critical magnetic field of about 25 T at 4.2 K. However, the mechanical behaviour is very poor, the material is brittle and severe degradation of the current density occurs with stress or bending. But the successful operation of Nb₃Sn magnets at about 12 T with about half a meter bore let grow the confidence in this material. The LCT coil from Westinghouse has a forced flow cooled Nb₃Sn conductor. The test of this coil will be crucial for the application of Nb₃Sn conductors in large coils for fusion reactors.

The radiation effects in Nb_3Sn differ considerably from those of NbTi owing to the long-range ordered atomic structure of the A15-phase. In compound superconductors, during the formation of the final structures, different types of atoms can exchange sites (i. e. disorder) or be slightly displaced from their original lattice site so as to significantly alter the electronic properties of the superconductor.

The nature of the defect or defects responsible for the degradation and restoration of both the superconducting and lattice properties of the A15 materials is not clear at the present time. On the one hand, site exchange disorder (replacement of A atoms by B atoms and vice-versa in the A_3B structure) has been identified as an important defect on the basis of x-ray and neutron diffraction studies. On the other hand, an "unknown defect", which may be associated with the loss of translational symmetry, has been suggested as a primary cause for the observable effects.

Early irradiation experiments of Cullen and Novak /52/ of Nb_3Sn samples in a fast neutron flux at 32 K show that the critical current was increased, but the increase was smaller the higher the initial value of J_c . The increase could be obtained for doses up to about 10^{18} n/cm² for samples of low initial J_c and for doses up to 3×10^{17} n/cm² for high initial J_c . With higher neutron doses the value of J_c decreased in each case. The value of T_c decreased by 0.18 K at 2.7×10^{18} n/cm². This behaviour of Nb_3Sn is confirmed by later irradiation experiments.

From the reported data, some conclusions can be drawn.

- Large decreases in the transition temperature T_c occur after doses at which the T_c of NbTi (and Nb) is essentially unchanged. Fig. 3-2 shows the ratio of the critical temperature T_c after irradiation to the critical temperature without irradiation for various A15 materials and for NbTi and Nb. A large decrease for A15 is seen being about 10 % at doses of about 10^{18} n/cm² and about 80 % for doses of some 10^{19} n/cm². At that dose NbTi shows no severe degradation in T_c . A T_c decrease, however, implies an effective J_c decrease, because J_c is generally measured at a fixed temperature T , and the value of J_c decreases as T approaches T_c . Therefore, reducing T_c is equivalent to measuring at a higher T , with a resultant decrease in J_c .

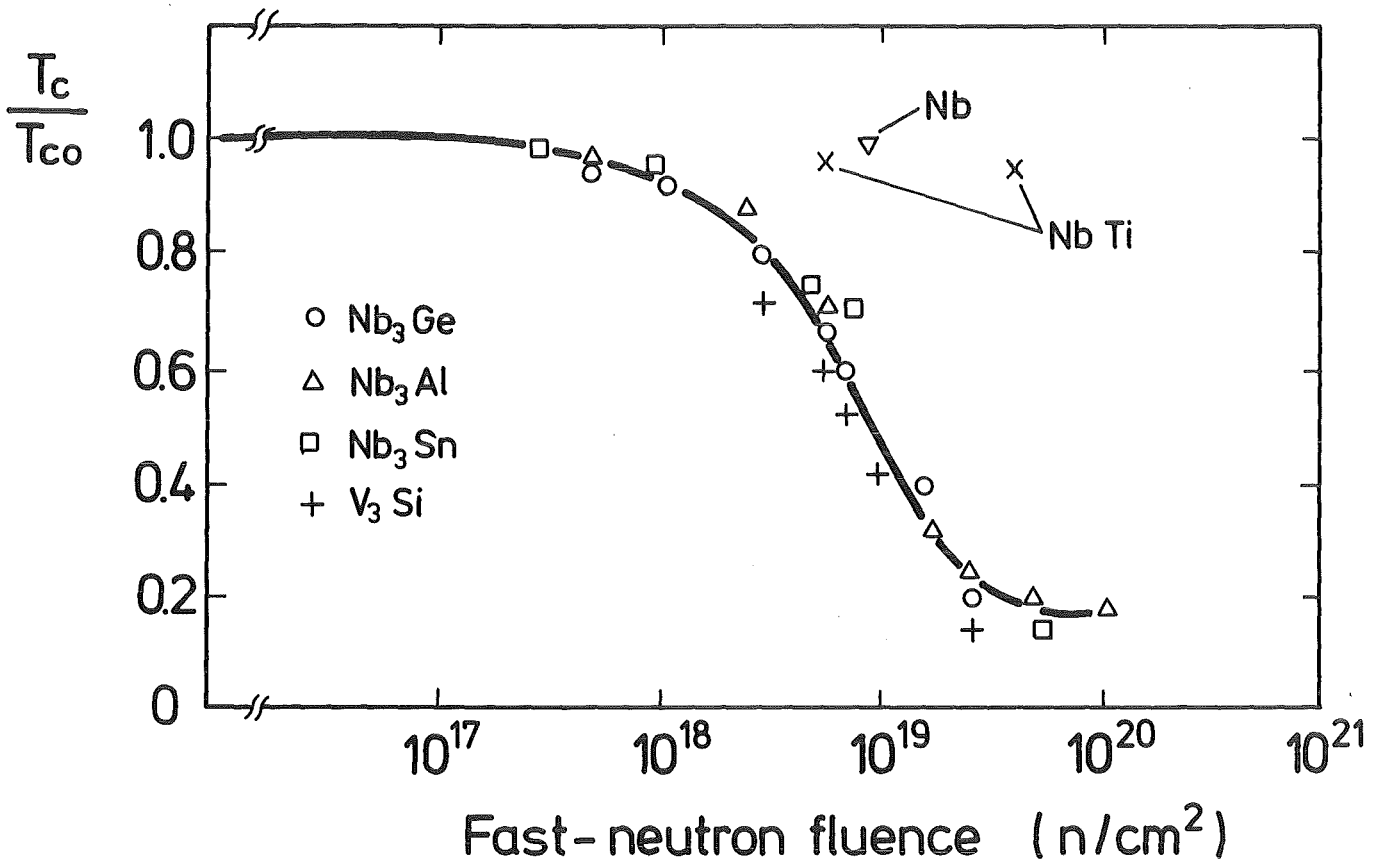


Fig. 3-2: Fractional change in critical temperature for various A15 and alloy superconductors (Nb, NbTi) after neutron irradiation at about 370 K /15, 50/.

T_c is also depressed following high energy neutron irradiation in non-stoichiometric alloys for deviations on either side of stoichiometry. At high fluences T_c approaches a saturation value between 2 and 4 K and the same final T_c value is reached irrespective of the initial composition of Nb_3Sn .

The transition temperature of the irradiated material is recovered with isochronal or isothermal anneals. In the isochronal anneals all the Nb-base compounds, independent of composition or fluence, start to show recovery of T_c between 400 - 500 °C. This annealing temperature is not applicable for fusion magnets.

- Although B_{c2} has not been as extremely studied as T_c for irradiated superconductors, several interesting features have emerged. For very low doses ($\sim 5 \times 10^{17}$ n/cm²), slight increases in $B_{c2}(0)$ have been observed for Nb_3Sn . This increase is most likely due to a slight increase in the normal state resistivity which overcompensates the decrease in T_c . For higher doses, $B_{c2}(0)$ decreases linearly with T_c , as is also observed for oxygen ion irradiated Nb_3Sn . Increases in B_{c2} for Nb_3Sn have also been observed in multifilamentary wires irradiated at low fluences ($< 2 \times 10^{18}$ n/cm²). Above this fluence B_{c2} decreases as T_c decreases.

The temperature dependence of $B_{c2}(T)$ for neutron irradiated Nb_3Sn has also been reported. The slopes of the critical field curves near T_c ($dB_{c2}/dT_c|_{T=T_c}$) are slightly enhanced over the unirradiated values.

- Extensive measurements on J_c changes due to neutron irradiation have been made. Fig. 3-3 shows the typical change of the normalized critical current density. This behaviour is clearly different from that of NbTi. The current density initially increases with increasing dose up to a factor of two and decreases then very steeply with furthermore increasing dose until the current capacity is completely destroyed. As design criterion the critical neutron fluence value (dose) in the decreasing slope where the current density reaches the initial value without irradiation is proposed.

Contrary to NbTi, this behaviour is even shown by optimized, i. e. high initial value of J_c (2×10^6 A/cm² at 4.2 K and 5 T), multifilamentary Nb_3Sn samples made by bronze technique.

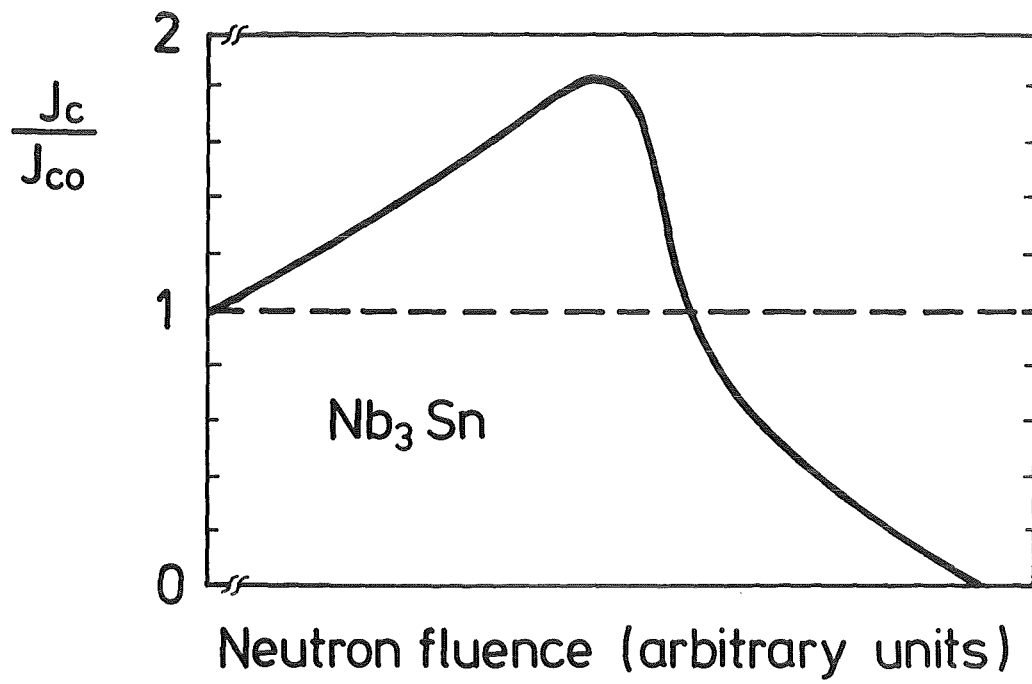


Fig. 3-3: Schematic of J_c/J_{c0} versus neutron fluence for Nb₃Sn.

At lower values of the applied field B the relative increase in $J_{c0}(B)$ is generally smaller for a given neutron dose and the fluence required for saturation of $J_c(B)$ is also smaller. This behaviour in $J_c(B)$ is interpreted in terms of flux pinning by radiation-induced defect cascades as well as changes in T_c and B_{c2} as the result of neutron irradiation.

In /45/ the critical dose for Nb_3Sn is given (defined as the point where $\Delta I_c = 0$ for 10 T) as 4.4×10^{18} n/cm² for a HFBR-spectrum ($E > 0.11$ MeV) and $(7.5 \pm 2.5) \times 10^{17}$ n/cm² for the 14 MeV RTNS-spectrum. (The damage energy is 0.19 eV/atom and the dpa's are 0.0019.) These doses are valid for multifilamentary wires.

3.4 Comparison of NbTi and Nb₃Sn

The main conclusions for the radiation behaviour of NbTi and Nb₃Sn should be summarized:

- A15 high field superconductors are more sensitive to neutron irradiation relative to other types of superconductor alloys.
- The influence of neutron irradiation on T_c and B_{c2} is very small for NbTi. At a dose of 10^{19} n/cm², T_c of NbTi is nearly unchanged while T_c for Nb₃Sn is decreased by 60 %.
- A fluence of the order of 10^{19} n/cm² (fission spectrum) produce only up to 20 % reduction of the critical current of NbTi in fields up to 6 T. But the same dose reduces the critical current for Nb₃Sn by about 95 %. Specially prepared Nb₃Sn specimens (single core) showed no degradation at 10^{19} n/cm².
- Irradiation data for Nb₃Sn with additions are not available.

It is recommended to use as design dose for superconductors used in fusion magnets a neutron fluence in the range of 1 to 5×10^{18} n/cm².

4. Neutron Irradiation Effects on Cu and Al

4.1 General

To provide an alternate path of the current when a superconductor is driven normal by any instability a low resistance material is required bonded to the superconducting material. The amount and the distribution of the material is designed so that the normal region in the superconductor cannot propagate and become superconducting again. This stabilization is provided in general by Cu or Al.

The stabilization material must transfer the Ohmic heat $R \cdot I^2$ generated in the affected region of the stabilizer to the coolant (I is the magnet current flowing in the stabilizer of resistance R). With the total heat transfer Q to the coolant the condition

$$Q \geq R \cdot I^2$$

must be fulfilled for cryogenic stabilization. An increase in the resistance R can be detrimental. Therefore a radiation induced resistance must be taken into account in the design of a fusion magnet.

The change of resistance is considered in terms of resistivity $\rho = R \cdot \frac{A}{l}$, where A is the cross section and l the length of the stabilization material. The resistivity of a material can be written as

$$\rho = \rho_0 + \rho(T) + \rho_M + \rho_D + \rho_T$$

Here is ρ_0 = residual (bulk) resistivity due to imperfections,

$\rho(T)$ = ideal lattice resistivity,

ρ_M = magnetoresistivity,

ρ_D = radiation induced resistivity due to lattice damage and

ρ_T = resistivity due to impurities produced by transmutations.

The residual resistivity can be increased by strain. The ideal lattice resistivity can be neglected at 4 K operation temperature, but not in the safety

integral for the protection of a superconducting magnet. The temperature dependence is clearly important for the design of normal conducting magnets. The magneto-resistivity depends generally not only on the magnitude of the magnetic field, but also on the impurity content, temperature, and details of the Fermi surface. The sum $\rho_{irr} = \rho_D + \rho_T$ is the radiation induced part in the expression for the total resistivity.

If the design shows that the tolerable resistivity increase is too large the following two solutions can be considered:

- Increase of the amount of stabilization material. This leads to a lower resistance $R = \rho \cdot l/A$ by enhancement of the cross sectional area of the stabilizer.
- Increase of shield thickness. That decreases the incident flux.

These solutions result in larger magnets.

A third possibility is the periodic warming up of the magnets to anneal partly or if possible totally the resistivity due to radiation induced at low temperatures. This has a serious economic impact.

Irradiation data of Cu and Al are reported in the review reports /1/ to /15/ and in references /24, 25/ and /53/ to /82/.

4.2 Neutron Irradiation Effects on Cu and Al

4.2.1 Radiation-Induced Resistivity in Cu and Al

A description of defects and defect production in metals is given in the book of Thompson /53/. Table 4.2-1 /1/ shows the resistivity $\rho = \rho_0 + \rho(T)$ for Cu, Cu alloys and Al for various temperatures. For high purity metals the residual resistivity ratio $\rho(300 \text{ K}) / \rho(4.2 \text{ K})$ is in the order of about 1000, while for ETP- or OFHC-Cu it is about 100 - 200. The latter value is usual for stabilizing Cu material in commercial superconductors. The residual (bulk) resistivity for 4.2 K varies more than an order of magnitude

Table 4.2-1: Resistivity of Cu, Cu alloys, and Al for various temperatures /1/

ρ [$n\Omega m$] at	4.2 K	21 K	78 K	300 K	Residual Resistivity Ratio ³⁾
Cu ETP ¹⁾ (annealed)	0.13	0.15	3.0	17.1	132
Cu OFHC ²⁾ (annealed)	0.16	0.18	2.6	17.2	108
Cu, pure (99,995 %)	0.0198	0.024	2.4	16.5	833
Beryllium Cu (2,5 % Be)	48	49.2	51.23	72.4	1.5
Beryllium Cu (1 % Be)	18.4	19.3	20.6	37.2	2.0
Chromium Cu (1 % Cr)	3.8	4.5	9.0	23.0	6.0
Zirconium Cu (0.15 % Zr)	1.35	1.8	5.6	19.0	14.0
Al, pure (99,998 %)	0.02	0.028	3.66	25.5	1275
Al, commercial electric grade (99,95 %)	1.01	1.1	4.0	25.5	25

1) ETP = Electrolytic Tough Pitch

2) OFHC = Oxygen Free High Conductivity

3) Residual Resistivity Ratio RRR = $\rho(300 \text{ K})/\rho(4.2 \text{ K})$

with the grade of Cu or Al as seen in table 4.2-1. It depends on impurities and defects. Their number are established during preparation of the raw stock and by the fabrication history of the conductor and winding of the coil package. During fabrication severe deformations occur producing defects. These must be removed by annealing at high temperatures ($> 200^{\circ}\text{C}$). The winding will be done at ambient temperature without any high temperature anneals, so a winding induced residual resistivity enhancement is stamped on the stabilizing material. Therefore this resistivity change must be controlled during the winding process to know the residual resistivity of the product. This allows to predict allowable resistivity changes by irradiation.

Several papers report radiation data at low temperatures. Table 4.2-2 shows resistivity changes of Cu during 5 K irradiation for various fluences of fast and/or thermal neutrons. Table 4.2-3 shows some data for Cu irradiated at 330 K and measured at 4 K for very high fluences up to 4.5×10^{19} fast neutrons per cm^2 . Table 4.2-4 shows resistivity changes for Al up to fluences of 10^{19} fast neutrons per cm^2 .

Fig. 4.2-1 shows the ratio of $\rho(300\text{ K})/\rho_{\text{irr}}$ versus the neutron fluence for Cu and low temperature irradiation. For the same fluence, fast neutrons are an order of magnitude more effective to produce defects than thermal neutrons. The straight line in the log-log-plot indicates that the radiation-induced resistivity is equal to the room temperature at a fluence of about 10^{20} n/cm^2 ($E > 0.1$ MeV). For a fluence of about 3×10^{18} n/cm^2 ($E > 0.1$ MeV) the radiation induced resistivity is about a tenth of the room temperature resistivity.

Fig. 4.2-2 shows the ratio of $\rho(300\text{ K})/\rho_{\text{irr}}$ versus neutron fluence for Al at low temperature irradiation. The slope of the straight line is higher than for Cu. Therefore the radiation-induced resistivity is equal to $\rho(300\text{ K})$ at a fluence of about 3×10^{19} n/cm^2 ($E > 0.1$ MeV). For a fluence of about $(1 - 2) \times 10^{18}$ n/cm^2 ($E > 0.1$ MeV) the radiation induced resistivity is about a tenth of the room temperature resistivity.

Careful inspection of Tables 4.2-2, -3, -4 shows that the data base for radiation effects is very poor. The data are valuable for defect production studies, but not very useful for the design of fusion magnets. The sample size is very small, typically a wire of a few cm length and a thickness of less than a mm. Most of the investigators consider only very high purity copper samples ($\text{RRR} \approx 1000$), but commercial Cu used as stabilization material will have a residual resistivity ratio of 100 to 200.

Table 4.2-2: Resistivity change of Cu due to low temperature neutron irradiation
 (with respect to the resistivity $n = 10^{-9}$; with respect to the fluence $n = \text{neutrons}$)

Sample Description	Residual Resistivity Ratio	Irradiation Temperature K	Preirradiation Resistivity nΩm	Postirradiation Resistivity nΩm	Neutron Fluence (Energy Spectrum) n/cm ²	/Reference/ (Year)
ASARCO (99.999 %) 5 cm long 0.25 mm Ø annealed	?	4.4	0.0155	0.0256	1.2×10^{16} (fission)	Coltman et al. /67/ (1962)
polycrystalline wire (99.999 %) 90 cm long 0.8 mm Ø annealed 2h, 1000 ^o C 0.5x10 ⁻³ mbar in air	$\rho_{290}/\rho_{3.2} =$ 5400	4.8	0.00314	0.00386	2.9×10^{16} (thermal)	Coltman et al. /68/ (1967)
wire, (99.999 %) 30 cm long 0.1 - 0.2 mm Ø annealed 1 h, ~700 ^o C at $p < 10^{-6}$ mbar	$\rho_{293}/\rho_{4.6} =$ 118 453	4.6	0.1422 0.0371	0.1623 0.0557	3.6×10^{16} (fission)	Burger et al. /75/ (1967)
polycrystalline wire, 49 cm long, 0.3 mm Ø, annealed 12 h, 800 °C, in vacuum	$\rho_{300}/\rho_{4.6} =$ 519 ($\rho_{300} = 16.97$ nΩm)	4.6	0.0327	0.9311	1.18×10^{18} (E>0.1 MeV)	Böning et al. /70/ (1970)
single crystal 64.1mm x 0.3mm x 0.26 mm	$\rho_{300}/\rho_{4.6} =$ 714	4.6	0.0238	0.8969	1.18×10^{18} (E>0.1 MeV)	

Table 4.2-2: Resistivity change of Cu due to low temperature neutron irradiation (continued)

Sample Description	Residual Resistivity Ratio	Irradiation Temperature K	Preirradiation Resistivity nΩm	Postirradiation Resistivity nΩm	Neutron Fluence (Energy Spectrum) n/cm ²	/Reference/ (Year)
polycrystalline wire, 5 cm long, 0.25 mm Ø	$\rho_{295}/\rho_{4.5} =$ 2280	4.5	0.00824	1.17024	2×10^{18} (E > 0.1 MeV)	Horak and Blewitt /71/ (1972)
wire (99.999 %) 15.4 cm long, 0.25 mm Ø annealed 16 h, 900 °C, 5x10 ⁻² mbar in air	$\rho_{295}/\rho_{10} =$ 492	18	0.038	0.958 1.308	1.23×10^{18} 1.83×10^{18} (E > 0.1 MeV)	Brown et al. /54/ (1974)
polycrystalline wires, 7.5 cm long 0.45 mm Ø annealed	$\rho_{295}/\rho_{4.5} =$ 882 987 2280	4.5	0.0192 0.0171 0.008	0.0242 0.406 1.162	5.7×10^{17} (thermal) 5.8×10^{17} (E>0.1 MeV) 2×10^{18} (E>0.1 MeV)	Horak and Blewitt /55/ (1975) /71/
polycrystalline wires (99.999 %) 31 cm long 0.17 mm Ø annealed 2 h, 700°C 5x10 ⁻⁴ mbar	$\rho_{295}/\rho_{4.6} =$ 432/1490 after anneal 432/1464 after anneal	4.6	0.01179 0.01202	3.226 3.231	8.49×10^{18} (E > 0.1 MeV) 8.49×10^{18} (E > 0.1 MeV)	Nakagawa et al. /62/ (1977)

Table 4.2-2: Resistivity change of Cu due to low temperature neutron irradiation (continued)

Sample Description	Residual Resistivity Ratio	Irradiation Temperature K	Preirradiation Resistivity nΩm	Postirradiation Resistivity nΩm	Neutron Fluence (Energy Spectrum) n/cm ²	/Reference/ (Year)
wire 2.6 cm long 0.12 mm Ø annealed	$\rho_{290}/\rho_{4.2} =$ 1432	4.2	0.01187	0.02137	4.5×10^{15} (15 MeV peak d-Be-neutrons)	Roberto et al. /72/ (1977)
	950	5	0.0178	1.356	2.52×10^{18} (E > 0.1 MeV)	Böning et al. (1970)
ASARCO (99.999 %) annealed 9×10^{-5} mbar in air	estimated 2180	4	0.0078	0.0575	1.8×10^{18} (thermal)	Williams et al., /56/ (1979)
wires (99.999 %) 0.1 mm Ø, annealed 2 h, 900 °C, 10^{-5} mbar same, but mechani- cally deformed (twisted)	≈ 900 ≈ 150	5	0.015 0.092	0.044 0.124	4.2×10^{16} (fission) 4.2×10^{16} (fission)	Takamura and Kato /24/ (1981)

Table 4.2-2: Resistivity change of Cu due to low temperature neutron irradiation (continued)

Sample Description	Residual Resistivity Ratio	Irradiation Temperature [K]	Preirradiation Resistivity [$n\Omega m$]	Postirradiation Resistivity [$n\Omega m$]	Neutron Fluence (Energy Spectrum) [n/cm^2]	/Reference/ (Year)
Commerical OFHC (99.95 %) 20 mm long 0.12 mm wide 25 μm thick partially annealed	$\approx 200-300$	4.2	0.0828	0.2436	7.25×10^{16} (14.8 MeV, RTNS)	van Konynenburg et al. /25/ (1983)
same, but 99.999 %	$\approx 200-300$		0.0949	0.2747	8.35×10^{16} (14.8 MeV, RTNS)	
unoxidized OFHC 1.1 cm long 0.126 mm \emptyset 1) recrystallized	363	4.2	0.0499	0.3533	RTNS-II (14.8 MeV) average flux	Guinan and van Konynenburg /60, 77/
2) 7.5 % cold-worked	153		0.1114	0.4249	$1.2 \times 10^{16} n/m^2s$	
3) 14.3 % cold-worked	91		0.1704	0.4805	no fluence given	

Table 4.2-3: Resistivity change of Cu (measured at 4 K) due to neutron irradiation at 330 K
(with respect to the resistivity $\rho = 10^{-9}$; with respect to the fluence $\Phi =$ neutrons).

Sample Description	Residual Resistivity Ratio (estimat.) ¹⁾	Irradiation Temperature K	Preirradiation Resistivity nΩm	Postirradiation Resistivity nΩm	Neutron Fluence (Energy Spectrum) n/cm ²	/Reference/ (Year)
ASARCO (99.999 %) annealed 9×10^{-5} mbar in air	(1900)	330	0.00894	0.9015	4.5×10^{19} (E > 1.0 MeV)	Williams et al. /56/ (1979)
same as above, but Cd-shield added ⁺	(2014)		0.00844	0.6679	4.5×10^{19} (E > 1.0 MeV)	<u>Note:</u> measured up to 5.1 T
Commercial magnet wire 0.25 mm Ø	(79)		0.2161	1.057	4.5×10^{19} (E > 1.0 MeV)	
same as above, but Cd-shield added ⁺	(82)		0.2067	0.9105	4.5×10^{19} (E > 1.0 MeV)	
ASARCO (99.999 %) annealed at 1000 °C in vacuum	(430)		0.03967	0.9409	4.5×10^{19} (E > 1.0 MeV)	
same as above, but Cd-shield added ⁺	(554)		0.03071	0.71	4.5×10^{19} (E > 1.0 MeV)	
⁺ to eliminate thermal neutron effects	¹⁾ assuming $\rho(300K) = 17 \text{ n}\Omega\text{m}$					

Table 4.2-3: Resistivity change of Cu (measured at 4 K) due to neutron irradiation at 330 K (continued)
 (with respect to the resistivity $\rho = 10^{-9}$; with respect to the fluence $\Phi =$ neutrons)

Sample Description	Residual Resistivity Ratio (estimat.1)	Irradiation Temperature K	Preirradiation Resistivity nΩm	Postirradiation Resistivity nΩm	Neutron Fluence (Energy Spectrum) n/cm ²	/Reference/ (Year)
ASR-Cu (99.999 %) annealed 2h, 1000°C at 10 ⁻⁴ mbar in air	$\rho_{300} / \rho_{4.2} = \approx 2000$ (1920)	330	0.00885	0.83	4.2 x 10 ¹⁹ (E > 1 MeV)	Chaplin and Coltman /59/ (1982)
same as above, but Cd-shield added ⁺	≈ 2000 (2038)		0.00834	0.83	12 x 10 ¹⁹ (thermal)	
ASR-Cu (99.999 %) annealed 2h, 1000°C at 3 x 10 ⁻⁶ mbar	≈ 500 (433)		0.0393	0.16	2 x 10 ¹⁹ (E > 1 MeV)	
same as above, but Cd-shield added ⁺	≈ 500 (559)		0.0304	0.16	2 x 10 ¹⁹ (E > 1 MeV)	
⁺ to eliminate thermal neutron effects: Note: all wires, 25 mm long, 0.25 mm Ø	1) assuming $\rho(300\text{ K}) = 17\text{ n}\Omega\text{m}$					

Table 4.2-4: Resistivity change of Al due to low temperature neutron irradiation
(with respect to the resistivity $\rho = 10^{-9}$; with respect to the fluence $\Phi = \text{neutrons}$)

Sample Description	Residual Resistivity Ratio	Irradiation Temperature K	Preirradiation Resistivity $n\Omega m$	Postirradiation Resistivity $n\Omega m$	Neutron Fluence (Energy Spectrum) n/cm^2	/Reference/ (Year)
wire, (99.999 %) 30 cm long 0.1 - 0.2 mm \emptyset annealed 1 h, 500 °C at $p < 10^{-6}$ mbar	$\rho_{293}/\rho_{4.6} =$ 1307 1058	4.6	0.0204 0.0252	0.0816 0.0853	3.6×10^{16} (fission)	Burger et al. /75/ (1967)
polycrystalline foil 44.2 μm thick 0.3 mm grain size annealed 15 h, 620 °C in air	$\rho_{300}/\rho_{4.6} =$ 1400 without size effect corr. = 2500 with size ef- fect correc- tion	4.6	0.021	3.1	2×10^{18} n/cm ² (E > 0.1 MeV)	Böning et al. /69/ (1969)
polycrystalline wire 5 cm length 0.25 mm \emptyset	$\rho_{295}/\rho_{4.5} =$ 2286	4.5	0.0102	3.824	2×10^{18} n/cm ² (E > 0.1 MeV)	Horak and Blewitt /71/ (1972)

Table 4.2-4: Resistivity change of Al due to low temperature neutron irradiation (continued)
 (with respect to the resistivity $\rho = 10^{-9}$; with respect to the fluence $\phi =$ neutrons)

Sample Description	Residual Resistivity Ratio	Irradiation Temperature K	Preirradiation Resistivity $n\Omega m$	Postirradiation Resistivity $n\Omega m$	Neutron Fluence (Energy Spectrum) n/cm^2	/Reference/ (Year)
polycrystalline wire 99.999 % 31 cm long 0.245 mm ϕ annealed 3 h, 500 °C in air	$\rho_{293}/\rho_{4.6} =$ after annealed 275/1351 275/1493 275/1470 275/1476	4.6	0.02052 0.01828 0.01832 0.01824	8.688 8.492 8.865 8.834	8.83 x 10 ¹⁸ 8.15 x 10 ¹⁸ 10.4 x 10 ¹⁸ 10.09 x 10 ¹⁸ (E > 0.1 MeV)	Nakagawa et al. /62/ (1977)
single crystal, high purity 50 mm long 13 mm ϕ	?	4.6	$(\rho_0) = ?$	$(\rho_0)+3.24$	1.6 x 10 ¹⁸ (E > 0.1 MeV)	Böning et al. /76/ (1977)
wire, (99.999 %) 0.3 mm ϕ annealed 2 h, 600 °C, at 10 ⁻⁵ mbar	?	5	$(\rho_0) = ?$	$(\rho_0)+0.0078$	4.2 x 10 ¹⁶ (fission)	Takamura and Kato /24/ (1981)

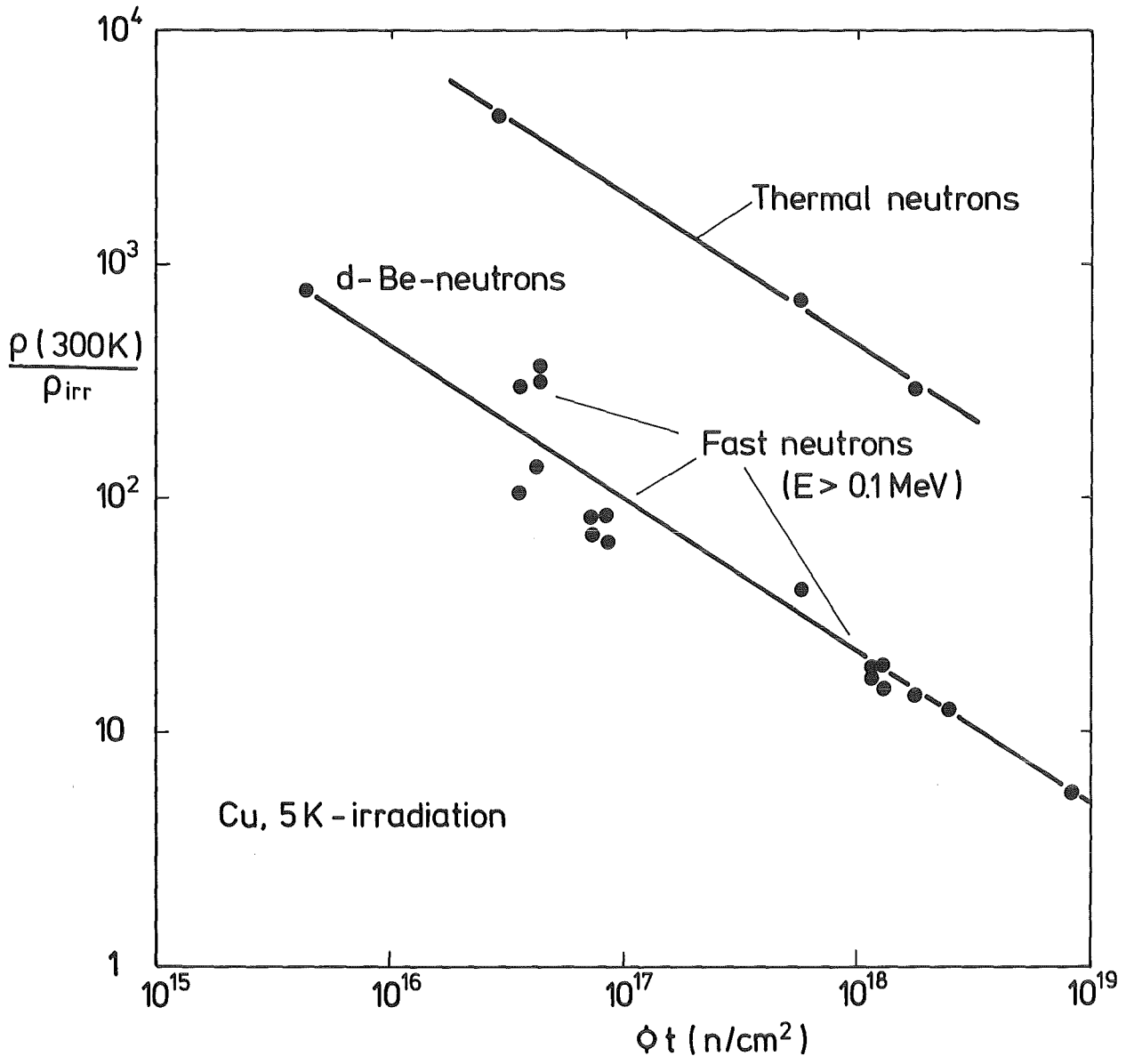


Fig. 4.2-1: Ratio of room temperature resistivity to resistivity after irradiation for Cu and low temperature irradiation.

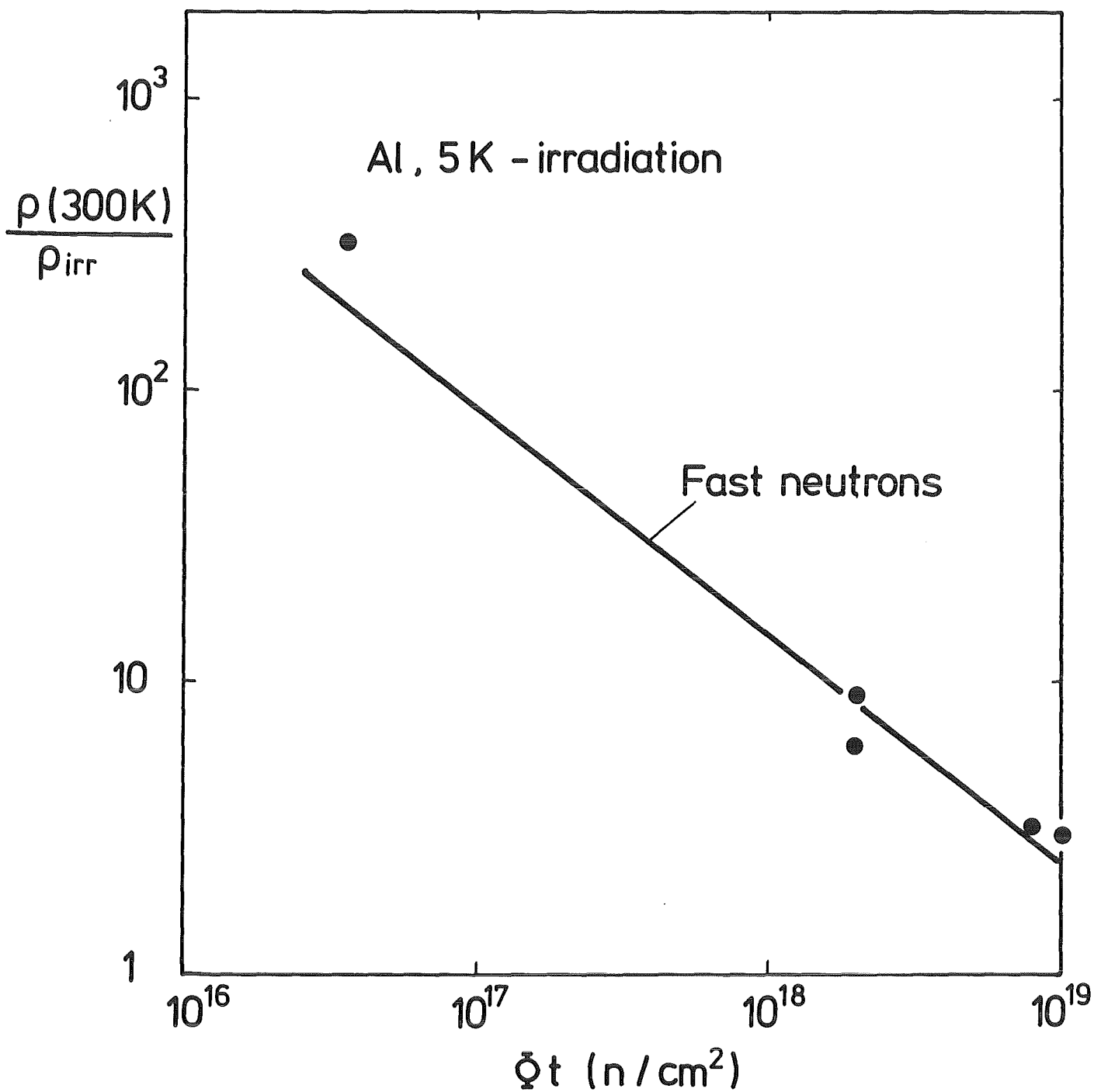


Fig. 4.2-2: Ratio of room temperature resistivity to resistivity after irradiation for Cu and low temperature irradiation

Fig. 4.2-3 /59/ shows the radiation-induced resistivity $\rho_{irr} = \rho_D + \rho_T$ versus the neutron fluence for copper with a residual resistivity of $\rho_0 = 0.00885 \text{ n}\Omega\text{m}$ (see also table 4.2-3). The effects due to defects and to transmutations are resolved. The increase in resistivity due to transmutations is linear, that due to defects falls off rapidly with increasing fluence. During the lifetime of water-cooled normal conducting copper magnets for fusion reactors the resistivity increase due to defects will be possible negligible compared to that resistivity produced by transmutations. If an extrapolation of the measured $\rho(\phi t)$ -dependence for the transmutations is justified, then the relation

$$\rho_T = \frac{5}{6} \times 10^{-21} (\phi t) \frac{\text{n}\Omega\text{m}}{\text{n}/\text{cm}^2}$$

can be derived from Fig. 4.2-3. A wall load of $1 \text{ MW}/\text{m}^2$ corresponds to a neutron flux of $4.43 \times 10^{13} \text{ n}/\text{cm}^2\text{s}$ (14.1 MeV neutrons). Then the fluence in 1 full power year (FPY) is $1.4 \times 10^{21} \text{ n}/\text{cm}^2$ and ρ_T would be $7/6 \text{ n}\Omega\text{m}$ per FPY and MW/m^2 for a normal conducting Cu coil near the plasma (or about 7 % of the room temperature resistivity).

4.2.2 Saturation Behaviour of the Defect Resistivity for Cu and Al

The Fig. 4.2-3 in the previous section indicates a saturation behaviour of the radiation-induced defect resistivity. That means, that irradiation generally increases the resistivity of a metal by ρ_D , but the rate of change in resistivity per unit fluence $d\rho_D/d(\phi t)$ decreases with increasing damage, resulting in a saturation value in the resistivity ρ_S . The concepts of initial damage rate $|d\rho_D/d(\phi t)|_0$ and saturation behaviour are described in /56/, resulting in

$$\rho_D = \rho_S [1 - \exp(-\alpha \cdot (\phi t))]$$

where the constant α is

$$\alpha = \frac{1}{\rho_S} \cdot \left| \frac{d\rho_D}{d(\phi t)} \right|_0$$

Values for α and ρ_S are given in the literature, but these values show no good accordance.

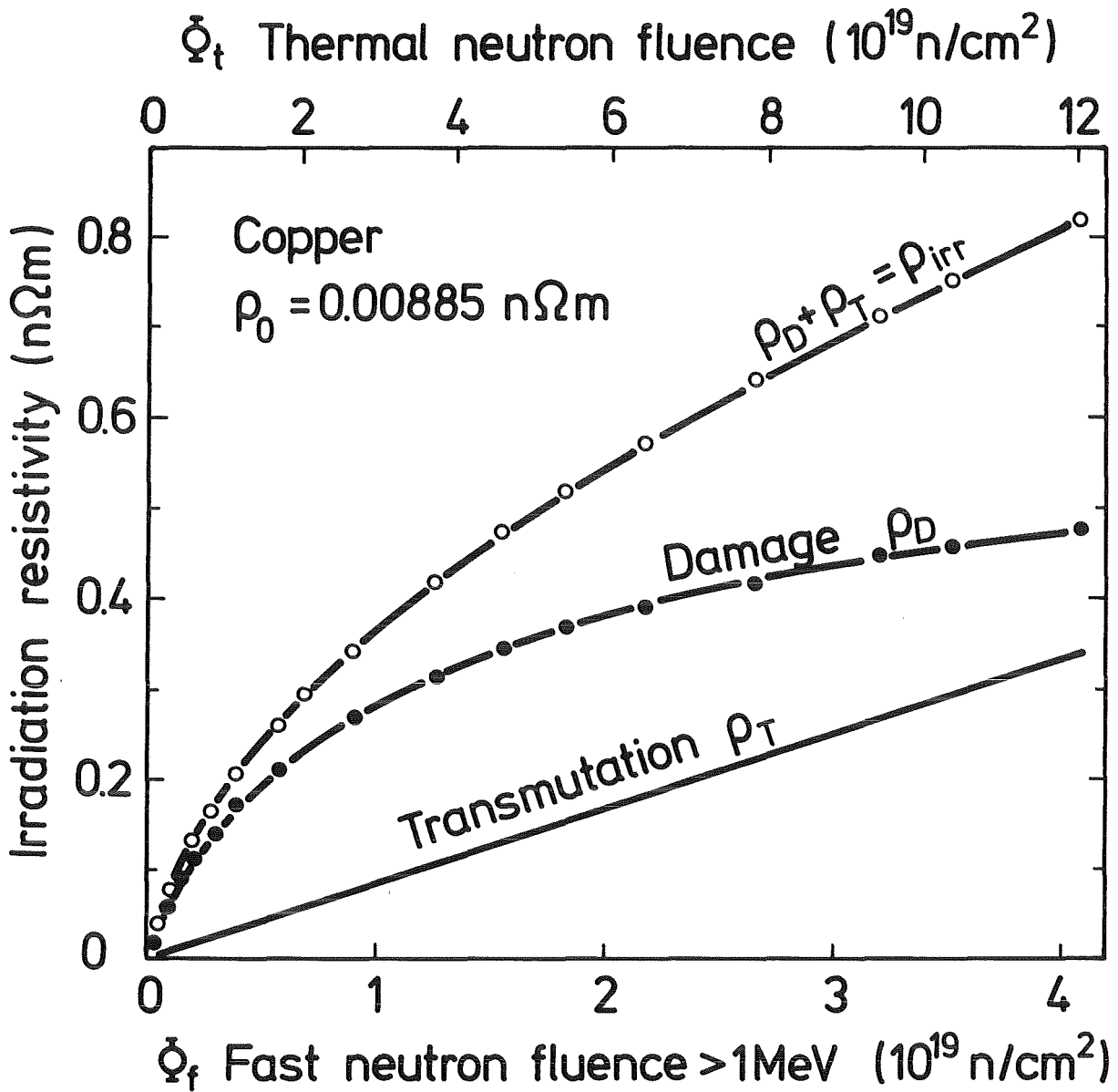


Fig. 4.2-3: Radiation induced resistivity increase versus thermal- and fast-neutron fluence. The resolved contributions due to damage and transmutation resistivity are shown for comparison (from 59).

For Al the range for ρ_S is 8 n Ω m to 9.55 n Ω m /15, 54, 55, 62, 64, 71/ and the initial damage rate varies from 14.9×10^{-19} n Ω m/n/cm² to 42×10^{-19} n Ω m/n/cm² /10, 62, 66, 67, 69, 71, 73/ depending on the irradiation energy spectrum of the irradiation facility and the accuracy of flux determination. The high initial damage rate is for high energy neutrons. In /57/, the initial damage rate is given to be 1520 n Ω m/dpa where dose and fluence is related by

$$\frac{D}{\text{Fluence}} = 1.465 \times 10^{-21} \frac{\text{dpa}}{\text{n/cm}^2} \text{ for Al.}$$

For Cu the range for ρ_S is 3 n Ω m to 4.38 n Ω m /15, 54, 55, 57, 62, 64, 71/ and the initial damage rate varies from 4.24×10^{-19} n Ω m/n/cm² to 25×10^{-19} n Ω m/n/cm² /10, 54, 62, 66, 67, 70, 71, 72, 73/ depending on the irradiation energy spectrum of the irradiation facility. High energy neutrons produce the high initial damage rate values. In /57/, the initial damage rate is given to be 649 n Ω m/n/cm² and the dose-fluence relation is

$$\frac{D}{\text{Fluence}} = 1.176 \times 10^{-21} \frac{\text{dpa}}{\text{n/cm}^2} \text{ for Cu.}$$

Table 4.2-5 summarizes the values found in the literature. Using the values in the table to calculate α one find for Al $\alpha = (1.56 - 5.25) \times 10^{-19}$ n Ω m/n/cm² and for Cu $\alpha = (0.97 - 8.33) \times 10^{-19}$ n Ω m/n/cm², where the lower values belong to a fission reaction spectrum and the higher values to high energy neutrons from d-Be or DT reactions. Using the ρ_D (ϕt) relation for Al with $\rho_S = 9$ n Ω m and $\alpha = 1.5 \times 10^{-19}$ /n/cm² /15/, the radiation-induced resistivity is 4.05 n Ω m for a fluence of 4×10^{18} n/cm². For Cu with $\rho_S = 4$ n Ω m and $\alpha = 1.0 \times 10^{-19}$ /n/cm² /15/ it is 1.32 n Ω m for the same fluence. This is valid only for low temperatures. At room temperature anneal changes the situation.

4.2.3 Annealing Behaviour

All recovery or annealing studies state in accordance that 100 % of the radiation-induced resistivity anneal(s) out in Al at room temperature, but only 80 - 85 % in Cu. That should be valid for successive irradiation after such anneals, but no experiments are published until now confirming this behaviour.

Table 4.2-5: Saturation resistivity ρ_S and initial resistivity change per unit fluence (initial damage rate) for Al and Cu.

	Al	Reference	Cu	Reference
ρ_S nΩm	8	/71/	3	/54/
	8.6	/64/	3.3	/71/
	9.0	/15, 54, 55/	3.4	/64/
	8.69 - 9.55	/62/	4.0	/15, 54, 55/
			3.53 - 4.38	/62/
$\left \frac{d\rho_D}{d(\phi t)} \right _0$ $\left 10^{-19} \frac{n\Omega m}{n/cm^2} \right $	14.9 ¹⁾	/66/	4.24 ¹⁾	/66/
	21.9 ²⁾	/66, 73/	6.4	/72/
	24.9	/71/	6.9	/71/
	29 - 32	/62/	7.23 ²⁾	/66, 73/
			7.5	/70/
	30 + 10	/10/	8 + 1	/10/
	39	/69/	8.7	/67/
	~ 40	/67/	9.2	/54/
	42 ³⁾	/66/	9 - 10	/62/
			21.1 ⁴⁾	/66/
			25 ³⁾	/66, 72/

- 1) VT53-Facility in the CP5-Reactor at Argonne National Laboratory.
- 2) Oak Ridge National Laboratory - Bulk Shielding Reactor - Low Temperature Irradiation Facility.
- 3) Lawrence Livermore National Laboratory - Rotating Target Neutron Source.
- 4) d-Be-neutrons.

If the induced resistivity exceeds the design value for a fusion magnet, it will be necessary to anneal the magnet periodically. Al has a two to three times larger rate of increase $d\rho_D/d(\phi t)$ than Cu, but anneals completely out at room temperature. Starting from the same bulk value of the resistivity, Al has to be annealed about three times more frequently than Cu. But Cu has a "residual radiation-induced resistivity" of about 15 - 20 %, so the anneals are not as "effective" as in Al. It is not known whether the residual radiation-induced resistivity adds up during cyclic anneals.

Due to the annealing behaviour discussed above the radiation-induced resistivity in normal conducting magnets operated at about 350 K is due to transmutations (see end of section 4.2.1) and doesn't anneal out.

4.2.4 Magnetoresistance

A complication of the situation is caused by the magnetoresistivity ρ_m for Cu and Al at low temperatures. Magnetoresistivity depends on the initial resistivity of the metal and the strength of the applied field. This dependence is often characterized in a Kohler plot suggesting that the total magnetoresistivity $\rho_m(B)$ can be reliably predicted from the applied field B and the resistivity in the absence of the applied field.

The magnetoresistivity for Cu and Al is shown in Fig. 4.2-4 /78/ and Fig. 4.2-5 /79/. Fig. 4.2-4 shows the magnetoresistivity for Cu and Al for different purities up to magnetic fields of 10 T, while Fig. 4.2-5 shows the magnetoresistivity up to 16 T for 3/4 hard OFHC Cu and high purity Al. It should be mentioned that the magnetoresistivity for Cu at low temperatures and magnetic fields higher than 10 T is about an order of magnitude larger than for Al.

In a Kohler plot the difference of the total resistivity with applied field B $\rho_m(B)$ and without field $\rho(0)$ divided by $\rho(0)$ is drawn as a function of $B/\rho(0)$

$$\frac{\rho_m(B) - \rho(0)}{\rho(0)} = f\left(\frac{B}{\rho(0)}\right)$$

where

$$\rho(0) = \rho_0 + \rho(T) + \rho_{irr}$$

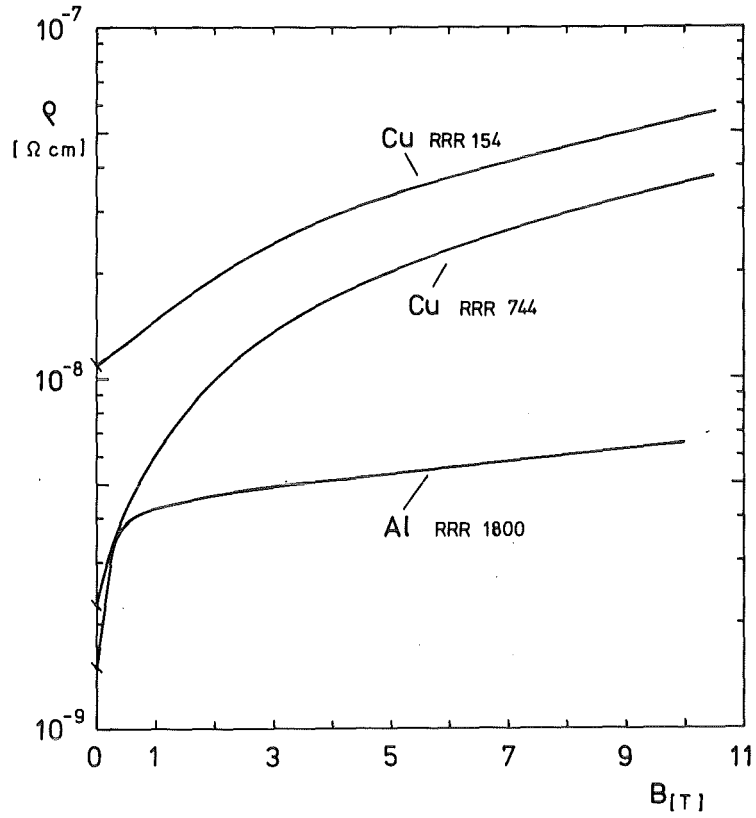


Fig. 4.2-4: The electrical resistivity of Cu and Al of different purities as a function of the applied magnetic field (up to 10 T) at 4.2 K /78/.

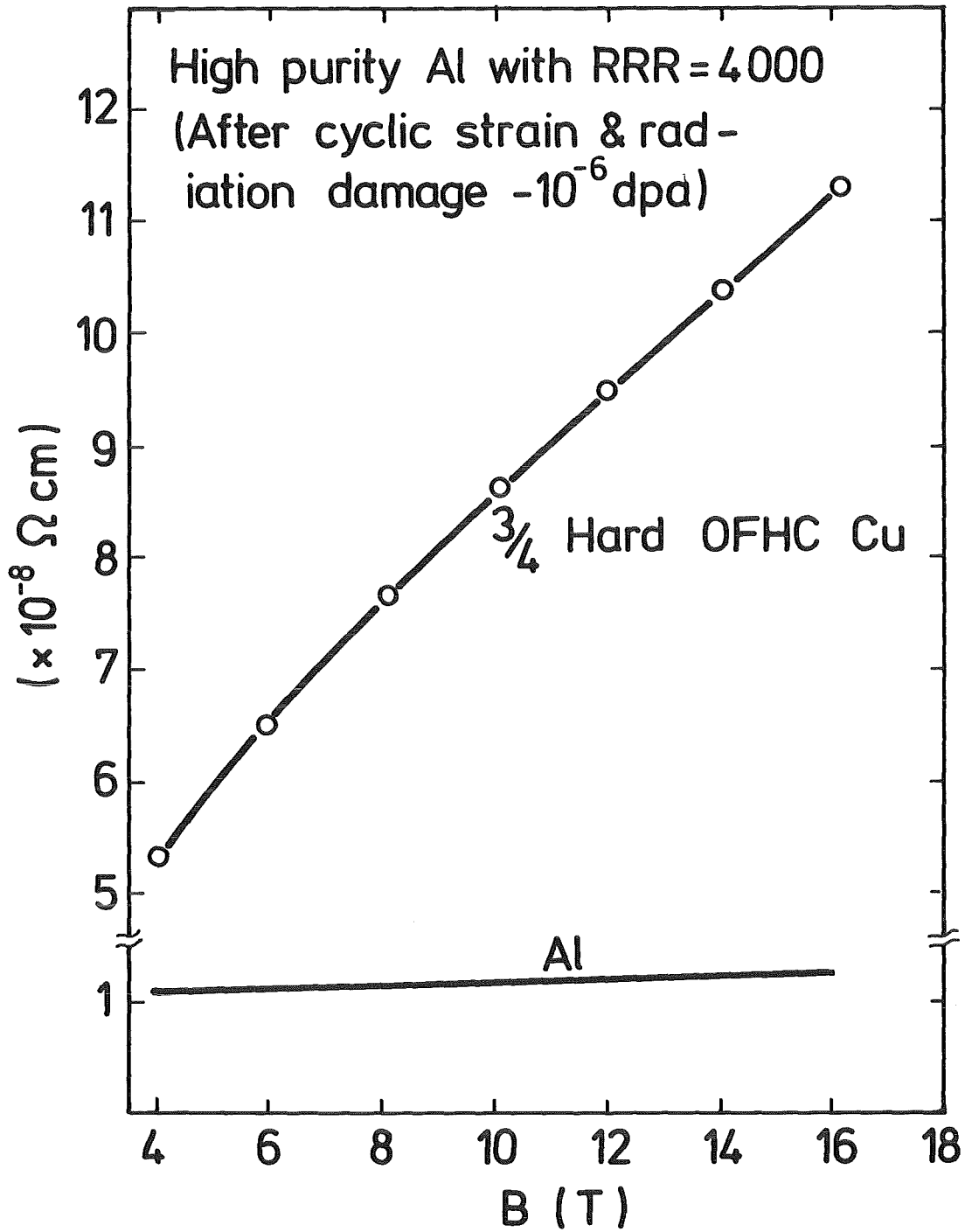


Fig. 4.2-5: Resistivity of High Purity Al and 3/4 Hard OFHC Cu as a function of the applied magnetic field (up to 16 T) /79/.

Fig. 4.2-6 /56/ shows a Kohler plot for Cu irradiated by reactor neutrons at 5 K and 330 K. The straight lines correspond to solutions of the form

$$\rho(B) = \rho(0) + 10^\alpha \cdot B^\beta \rho(0)^{1-\beta}$$

where α and β are the intercept and slope, respectively, of one of these lines on the Kohler plot [B in T, ρ in $n\Omega m$].

Fig. 4.2-7 /57/ shows magnetoresistivity Kohler curves for Al after reactor-neutron damage at 4.6 K. The curves show a strong bend-over to saturation at high values of $B/\rho(0)$, no deviation from Kohler's rule during damage production, and only a modest deviation (compared to Cu) for any and all of the partially annealed states. All of these Al data are for a single sample. Therefore, it is not known whether a variety of samples would lead to a broader band of Kohler curves, as it was the case with Cu. A computer fit of the data gives:

$$\rho(B) = \rho(0) + \rho(0) \cdot 10^a \left| 1 - \frac{1}{1+z} \right|^b$$

with

$$z = 10^d \left| \frac{B}{\rho(0)} \right|^c$$

The parameter values a , b , c , d are:

	a	b	c	d
A (as-damaged)	0.17	1.73	1.1	-0.7
B (partially annealed)	0.34	1.77	1.1	-0.9

The fits are seen in Fig. 4.2-7 b. Based on these data for the magnetoresistivity and the saturation behaviour a comparison for Al and Cu was made. Fig. 4.2-8 /57/ shows the result. Such detailed data on commercially available stabilizer material is exactly what is needed in order to access the relative merits of Cu versus Al. Al has a larger saturation resistivity (by a factor of about 2 to 2.5), and a larger resistivity increase with dose. But Cu has a larger magnetoresistance than Al (by a factor of about 10 at high fields) and anneals not fully out at room temperature (only

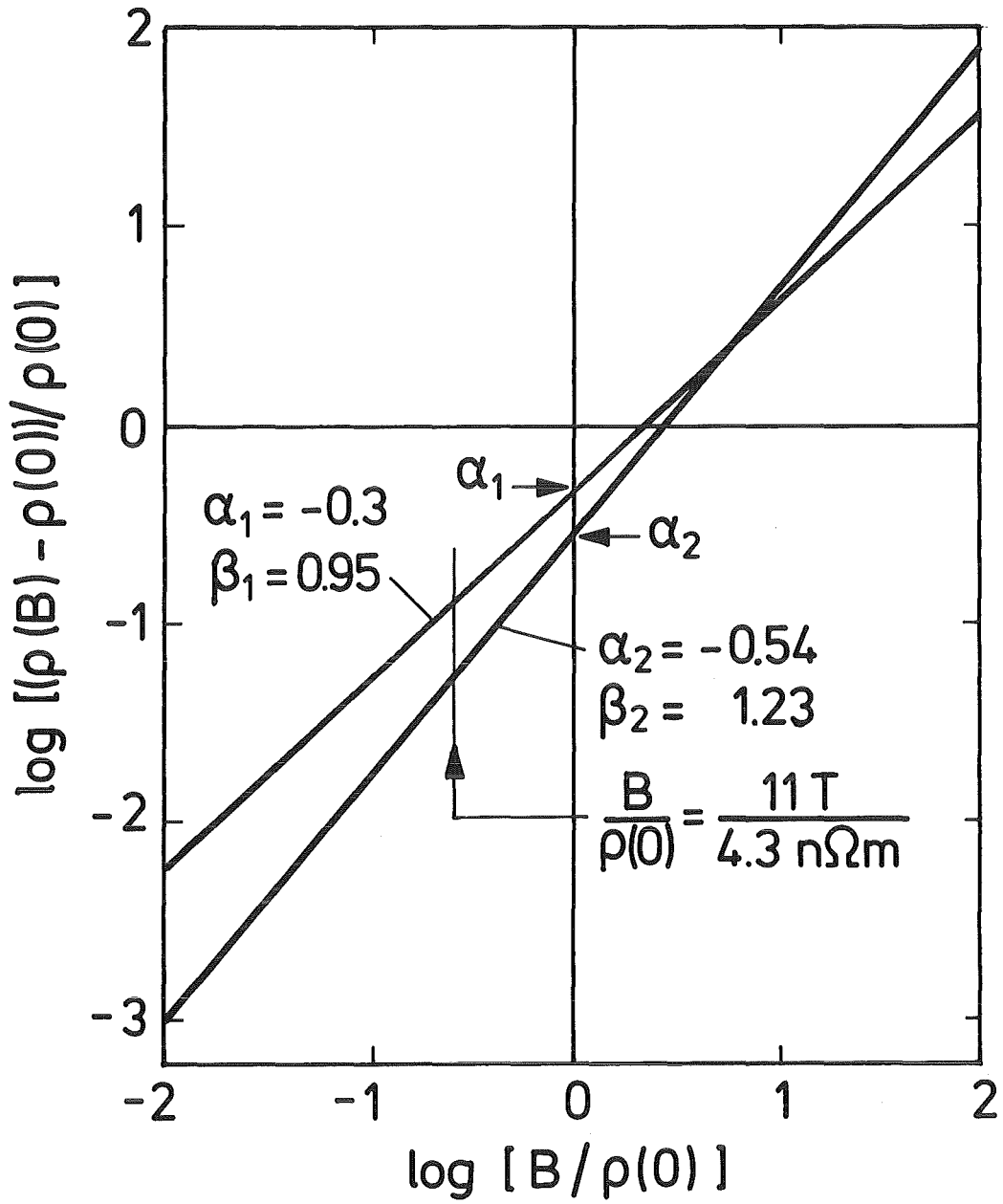


Fig. 4.2-6: Kohler plot for Cu irradiated by neutrons at 5 K and 330 K /56/. The α 's and β 's are the intercepts and slopes of the envelope lines. More than 1200 points are enclosed by the envelopes.

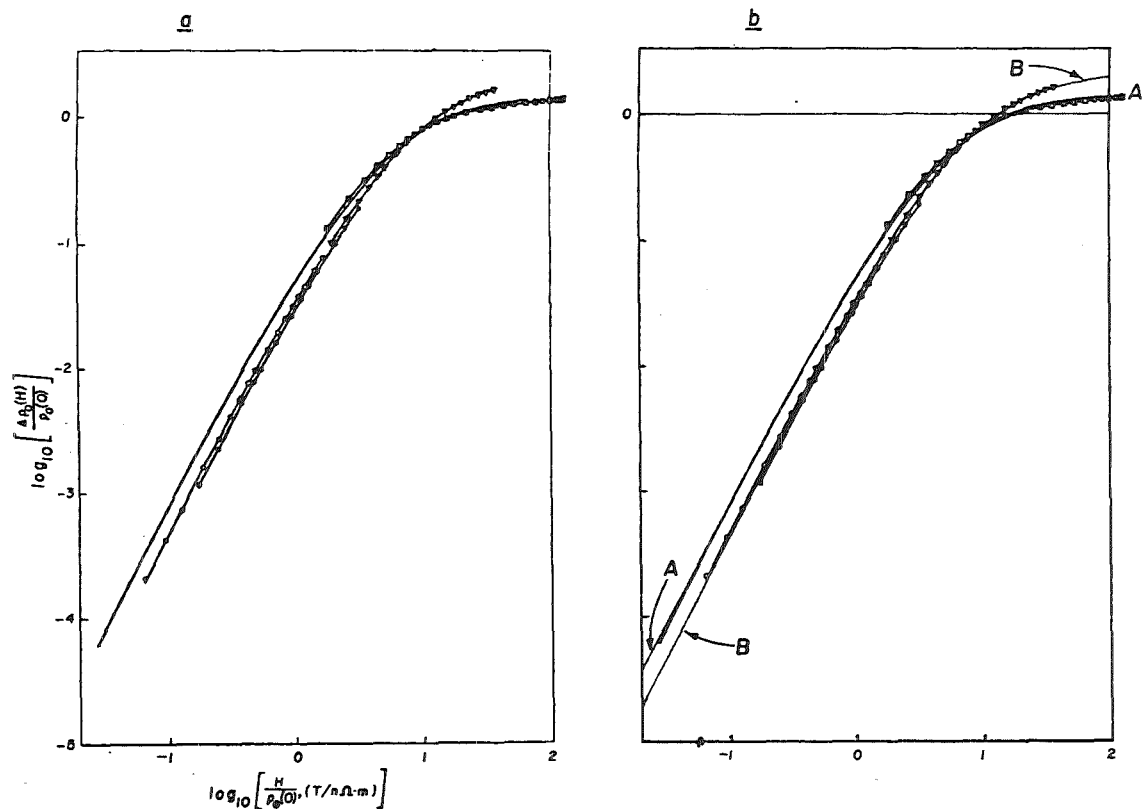


Fig. 4.2-7: Aluminum magnetoresistivity Kohler curves after reactor-neutron damage at 4.6 K.

(a) Copied from Ref. /69/. The solid curve without data points summarizes all as-damaged data over more than two orders of magnitude of defect concentration. The data points nearly coincident with this curve are for 'complete' recovery after anneal at 350 K. The other curves with data points represent stages of partial recovery and deviate most from the as-damaged curve after anneals between 80 and 200 K.

(b) Same as (a) with addition of two computer-fitted and drawn curves. Curve 'A' is fitted to the as-damaged curve, and 'B' approximates the partially recovered data curves. These curves are copied from Ref. /57/.

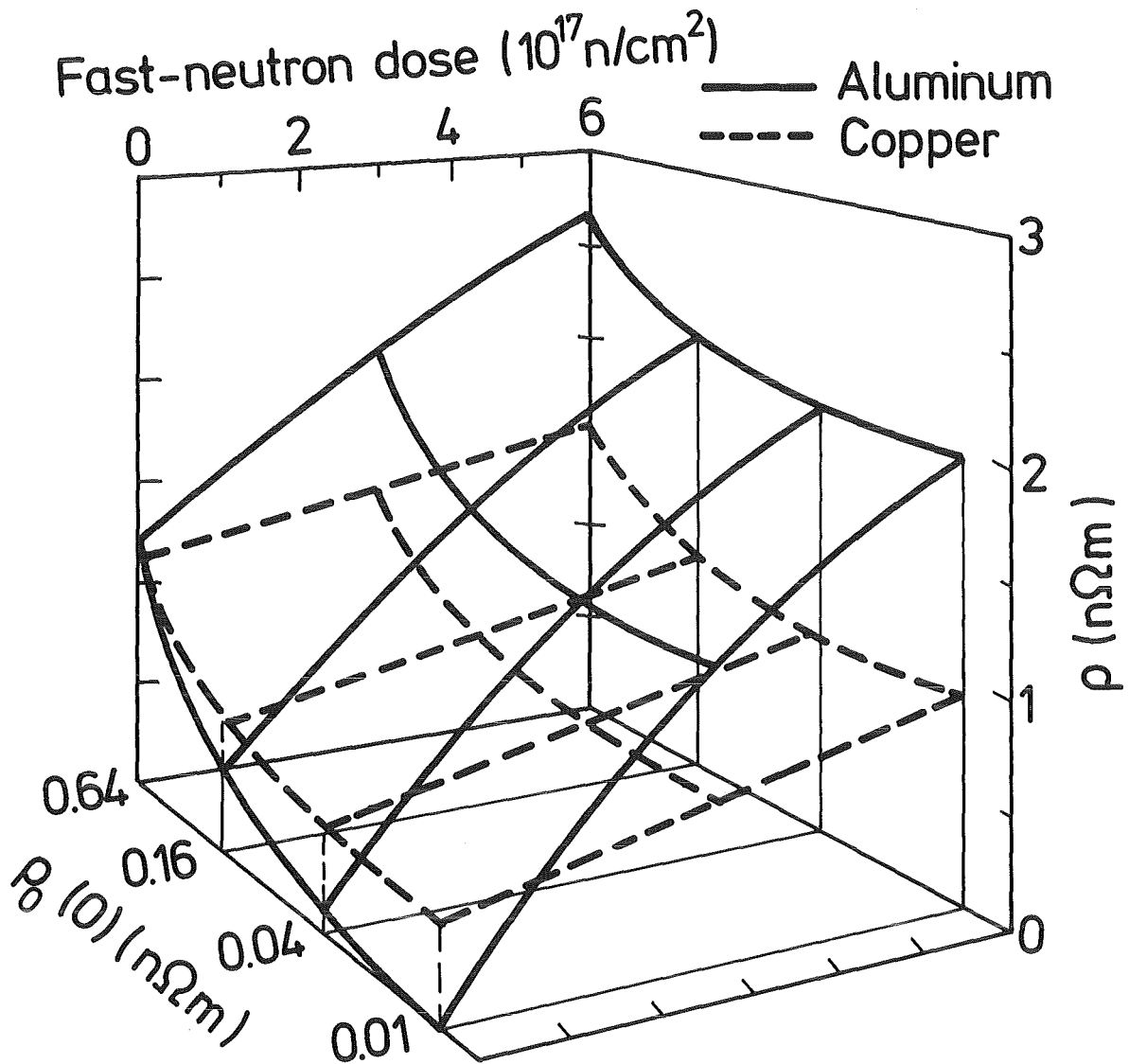


Fig. 4.2-8: Typical change in total resistivity ρ in Al and Cu at $B = 10 \text{ T}$ for different initial values of resistivity $\rho(0)$ under various irradiation conditions (Ref./57/). $\rho(0)$ was varied by using commercial and high-purity material and by performing various annealing treatments.

80 - 85 %). Fig. 4.2-8 shows that Al is better in the region of low doses ($\leq 1 \times 10^{17}$ n/cm²) and high purity (low bulk resistivity $\rho_0(0)$). More experimentally generated curves of this type need to be produced at 4.2 K with the neutron spectrum expected at the fusion magnet (such as by a combination of fission and 14 MeV neutrons) and at high fields (~ 12 T).

In /77/ the changes which occur in the magnetoresistivity of copper samples (having various purities and pretreatments) have been measured at magnetic fields up to 12 T during the course of sequential fusion neutron (14.8 MeV) irradiations at about 4 K and anneals to room temperature. The results involving the variation of zero field resistivity by cold work, irradiation, and repeated irradiation and anneal cycles fall on a single Kohler line to within ± 2 % as shown in Fig. 4.2-9. This fact greatly simplifies the task of predicting the response of the magnetoresistivity of actual conductors to changes resulting from fabrication of magnets and use in fusion reactors. But more curves of this type are needed for commercial materials.

4.2.5 Mechanical Properties

Mechanical properties of copper are known to change when exposed to neutron irradiation. The yield stress in Cu increases during irradiation with a fission-neutron spectrum. Fig. 4.2-10 shows the yield stress versus neutron fluence for the irradiation temperatures 4.2 K, 78 K and 300 K. The increase in the yield stress is about a factor of ten for doses raising from 10^{16} n/cm² to 10^{20} n/cm². Similar experiments with fusion neutrons have not been performed. Embrittlement, fatigue, and creep are not serious at the anticipated doses ($\leq 10^{19}$ n/cm²), and the effect of the irradiation on the mechanical properties of the stabilizing material is not considered important for outside coils. However, the change of mechanical properties will be important for near plasma coils, where higher fluences occur.

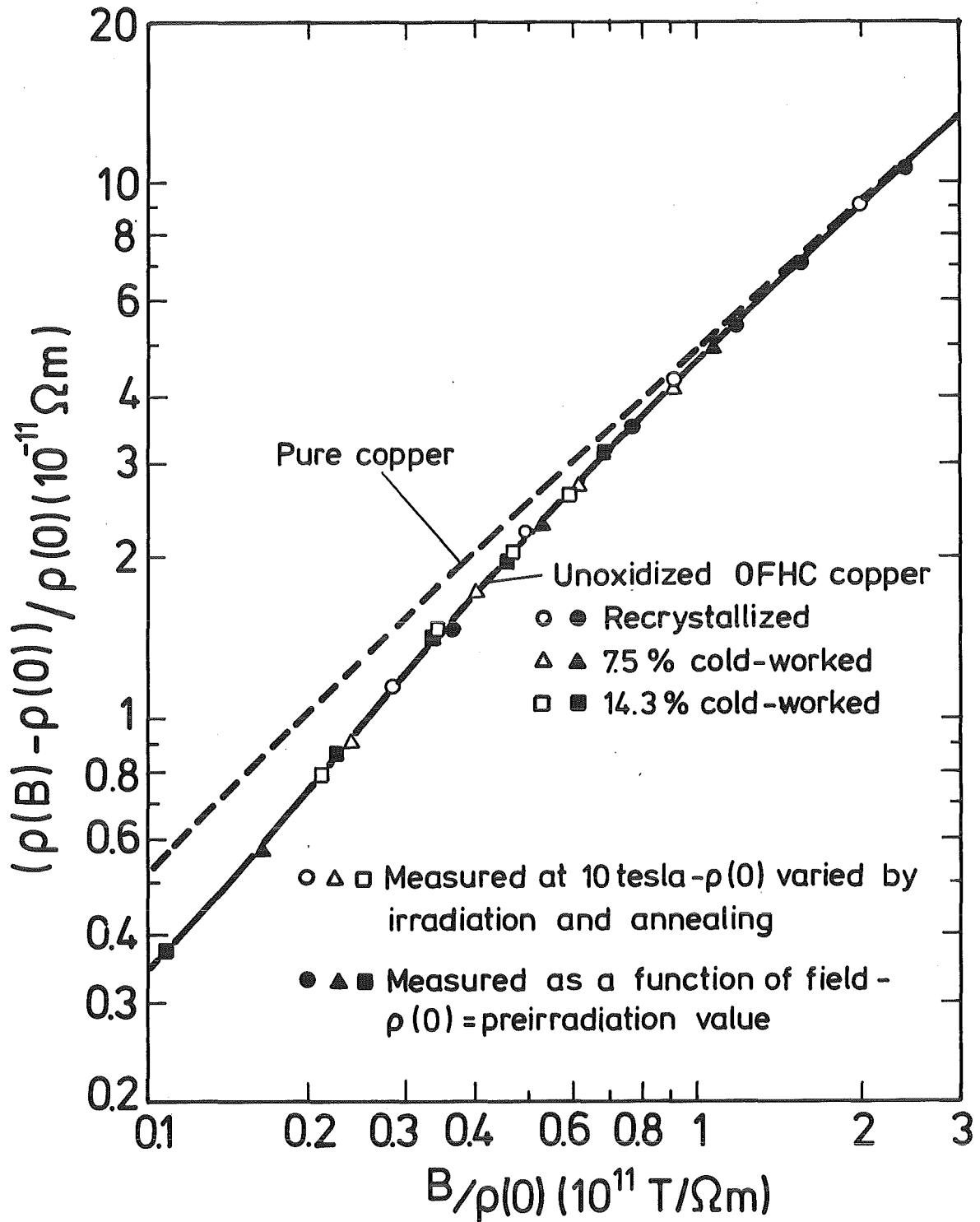


Fig. 4.2-9: Kohler plot for unoxidized OFHC copper. The dashed line is from F. R. Fickett, 4th Int. Conf. on Magnet Techn., BNL, CONF-720908, Brookhaven, N.Y. (1972), p. 539.

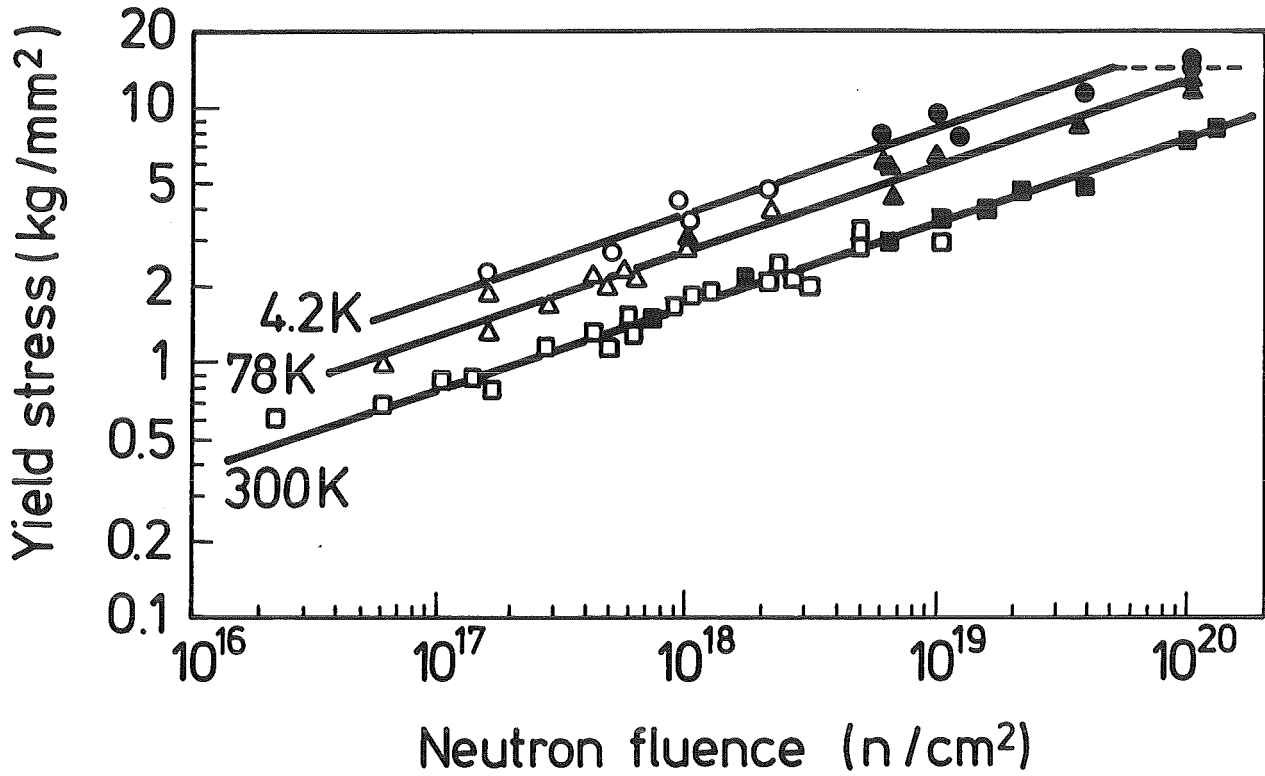


Fig. 4.2-10: Effect of neutron irradiation on the yield stress of Cu at various temperatures. The yield stress is plotted as a function of the fluence. The slope of the straight lines is 1/3. Open symbols: bombarded in graphite reactor; closed symbols: bombarded in LITR /63/.

4.2.6 Conclusions

- At present the behaviour of actual stabilizing material at high fields and high doses can only be predicted by extrapolation, rather than by any close comparison with existing data.
- The biggest uncertainty in specifying the amount of copper in a given cross section of conductor is the amount of recovery that results from repeated annealing after interim exposures to neutron irradiation at 4.2 K. More experiments are needed.
- The initial resistivity of the stabilizer when the magnet is first operated will depend on impurity levels and winding strain which may vary locally along the length of the conductor. Quality and process controls during manufacture of the magnet are the primary factors in obtaining predictable initial resistivity and magnetoresistivity in the stabilizer. Together with the resistivity design limit the allowable radiation - induced resistivity can be predicted.
- A "hot spot in the superconductor" (local transition from superconducting to normal conducting state) is cooled through the stabilizing material. Therefore, the effect of irradiation on the thermal conductivity κ of the stabilizer is a necessary information for conductor designs. From data on ρ increase an irradiation-induced decrease in κ can be calculated by the Wiedemann-Franz law $\rho \cdot \kappa = \text{const}$. But, the applicability of that law to low temperature fast-neutron irradiation in a stabilizing material should be investigated.

5. Composite Superconductors

As discussed in section 4.1 the condition $Q \geq R \cdot I^2$ must be fulfilled for cryogenic stabilisation (Q = heat transfer to the coolant, R = resistance, I = transport current). This relation can be replaced by the MADDOCK-criterion /83/

$$J \leq \left| \frac{Q_c k}{\rho} \right|^{2/3} \frac{1}{I^{1/3}}$$

where

- J = current density in the stabilizer
- Q_c = maximum heat flux which can be transferred to the coolant helium ($\sim 0.3 \text{ W/cm}^2$ for bath cooling)
- I = transport current
- ρ = resistivity
- k = geometrical factor, defined by $P = k \cdot \sqrt{A}$ where P is the wetted perimeter

Another design criterion for a conductor is the protection of the coil. This condition can be written as /83, 1/:

$$J \leq \left| f(\theta_m) \cdot \frac{V_m \cdot I}{E_s} \right|^{1/2}$$

where

- V_m = maximum induced voltage
- I = transport current
- E_s = stored energy
- J = current density in the stabilizer
- $f(\theta_m)$ = temperature integral

The temperature integral is defined as:

$$f(\theta_m) = \int_{\theta_b}^{\theta_m} \left(\frac{\gamma c}{\rho} \right) d\theta$$

where

- θ_b = bath temperature
- θ_m = maximum reached temperature
- γ = mass density
- c = specific heat of the normal metal
- ρ = resistivity

Both criteria show that an enhancement of the resistivity decreases the maximum attainable current density.

Okada and Hayashiuchi /5/ analysed the effect of neutron irradiation on a composite superconductor based on assumptions that the overall current density is determined by cryogenic stabilization and based on the available data of the alloy and compound superconductor together with the resistivity of the stabilizing material.

For Cu stabilized NbTi conductor the maximum transport current density decreases monotonically mainly regulated by the stabilizing effects through resistivity change by neutron irradiation.

For Cu or Al stabilized Nb₃Sn the maximum transport current density falls more steeply near the fluence region of 10^{19} n/cm² because of the changes in the superconducting properties. The behaviour can be explained by considering the T_c degradation, which decreases J_c in Nb₃Sn by neutron irradiation. Results of Nb₃Sn discussed in the preceding chapter show that the critical current of Nb₃Sn wires is enhanced over the unirradiated values for doses below about 10^{18} n/cm² and that the enhancement is higher at higher field values. Above 5×10^{17} n/cm² the rapidly decreasing T_c dominates, which causes I_c to degrade rapidly.

Soell /13/ calculated the maximum magnetic induction values B_m for different toroidal coil systems taking into account the radiation-induced changes. The critical data of NbTi, Nb₃Sn and the resistivity of copper and aluminum are considered as parameters. The criteria for full stability and for coil protection under the influence of radiation damage are discussed. The result is shown in Fig. 5-1.

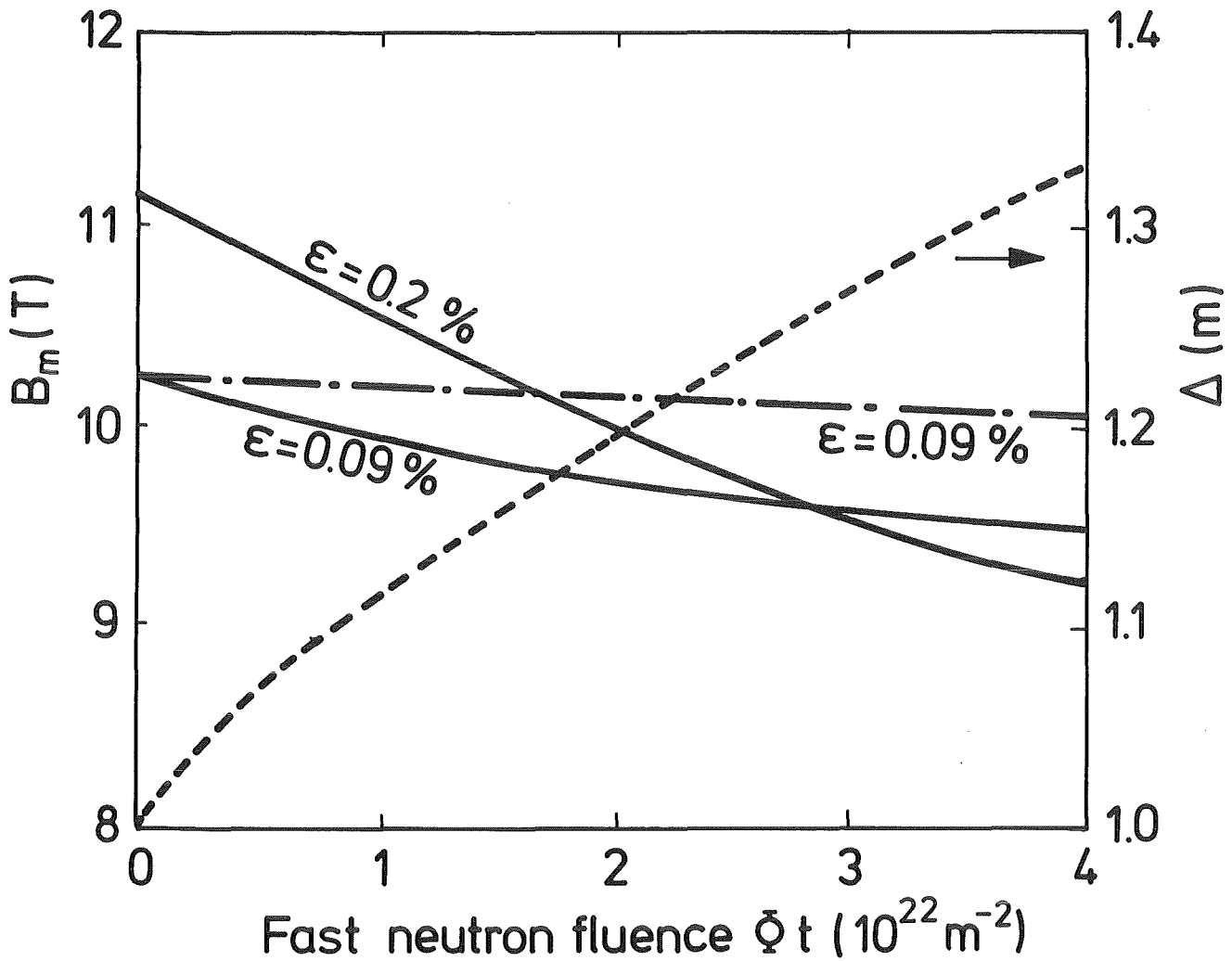


Fig. 5-1: Dependence of the maximum magnetic induction B_m on the neutron fluence for the T1 system ($r_1 = 4 \text{ m}$, $r_2 = 14 \text{ m}$, $\Delta = 1 \text{ m}$) produced by (—) increase of radiation induced resistivity in copper, (----) decrease of the critical current density in the superconductor (Nb_3Sn). The dotted line shows the increase of the winding thickness necessary to fix the B_m value given by unirradiated copper for a design strain $\epsilon = 0.09\%$ (from 13).

Comparing the changes in J_c versus dose for both NbTi and Nb₃Sn with property changes for the other magnet components, it is obvious that radiation effects in the bulk of the superconductor will probably not be the limiting radiation problem. In the case of composite NbTi conductors the overall current density is mainly limited by the radiation-induced increase in resistivity of the stabilizing normal conductor. For Nb₃Sn, however, the radiation-induced degradation of the superconducting properties (T_c and J_c) is possibly dominating the effects of the stabilizing material.

The alloy superconductor NbTi will not be the critical component of a fusion magnet. But the data are achieved in experiments which do not fully represent the conditions to be expected for a fusion magnet.

The main problem to be addressed by the magnet designers is the "hot spot" question with respect to irradiation behaviour mentioned at the end of section 2. It should be noted that severe degradation of J_c with stress or bending in a superconducting magnet may be the limiting effect for the Nb₃Sn conductor.

The irradiation effects on cupronickel, which is widely used as a matrix material, can be neglected. Irradiation effect on the metallic bond between superconductor and normal metal is also of concern. In the intermetallic layer between the superconductor and the normal metal matrix, which is composed of ternaries of Nb, Ti and Cu generally a high thermal and electrical resistivity is encountered. The bond is responsible for a somewhat lower thermal diffusivity from the superconductor to the matrix. The intermetallic diffusion layer between the superconductor and the matrix is increased, when the composite conductor is exposed to nuclear irradiation. Thus at an unchanged magnetic diffusivity the thermal diffusivity is further reduced. At present, measurements on thermal diffusivity over the intermetallic barrier are nonexistent due to the complexity of the problem.

Acknowledgements

It is a pleasure to thank the staff of FIZ/4 (Fachinformationszentrum Energie, Physik, Mathematik, GmbH, Eggenstein-Leopoldshafen) for the support in the literature research.

References

- /1/ H. Brechna, Superconducting Magnet System, Springer-Verlag, 1973, Chapt. 4.9, p. 339-351.
- /2/ H. Brechna, W. Maurer, Irradiation Effects in Superconducting Synchrotron Magnets. KfK-1468, 1971, and Proc. of the 8th Int. Conf. on High-Energy Accelerators, CERN 1971, pp. 224-227.
- /3/ G. M. McCracken, S. Blow, The Shielding of Superconducting Magnets in a Fusion Reactor. CLM-R 120, 1972.
- /4/ W. Schilling et al., Proc. of the Int. Conf. on Vacancies and Interstitials in Metals. Jülich 1968, pp. 255-361.
- /5/ T. Okada et al., Neutron Irradiation Effects on Superconducting Nb-Ti Alloys in the Magnets for Fusion Reactors. In Radiation Effects and Tritium Technology for Fusion Reactors. CONF-750989, Vol. II, pp. II.436-II.457, 1976.
- /6/ M. Soell et al., The Influence of Low Temperature Neutron Irradiation on Superconducting Magnet Systems for Fusion Reactors. IEEE Trans. on Magnetism, Vol. MAG-11, No. 2, March 1975, pp. 178-181.
- /7/ M. A. Abdou, Radiation Considerations for Superconducting Fusion Magnets. J. of Nucl. Mat. 72 (1978), pp. 147-167.
- /8/ M. Soell, The Influence of Radiation Damage on the Properties of a Superconductor. IPP 4/104, 1972 (in German).
- /9/ N. N. Mikhailov et al., Einfluß von Strahlenschäden auf die Eigenschaften technischer Supraleiter. KfK-tr-465, "I. V. Kurchatov"-Institut für Atomenergie, IAE-2292, Moskau 1973.

- /10/ J. F. Guess et al., A Survey of Radiation Damage Effects in Superconducting Magnet Components and Systems. ORNL-TM 5187, 1975.

- /11/ H. Ullmaier, Radiation Damage in CTR Magnet Components. In Radiation Effects and Tritium Technology for Fusion Reactors. CONF-750989, Vol. II, pp. II.403-II.421, 1976.

- /12/ W. Heinz, E. Seibt, Radiation Damages in Superconducting Materials. 6th Int. Conf. on Magnet Techn., Bratislava, 1977.

- /13/ M. Soell, Influence of Radiation Damage on the Maximum Attainable Magnetic Field for Toroidal Fusion Magnet Systems. J. of Nucl. Mat. 72 (1978), pp. 168-176.

- /14/ S.T. Sekula, Effect of Irradiation on the Critical Currents of Alloy and Compound Superconductors. J. of Nucl. Mat. 72 (1978), pp. 91-113.

- /15/ B. S. Brown, Radiation Effects in Superconducting Fusion-Magnet Materials. J. of Nucl. Mat. 97 (1981), pp. 1-14.

- /16/ H. W. Weber, Neutron Irradiation Effects on Alloy Superconductors. J. of Nucl. Mat. 108 + 109 (1982), pp. 572-584.

- /17/ M. Soell, Influence of Radiation Damage to Superconducting NbTi Coils for Fusion Reactors. Proc. of the 7th Symp. on Fusion Technology, Grenoble, 1972, pp. 311-318.

- /18/ M. Soell, Superconducting Magnet Systems for Fusion Reactors, Kerntechnik 19. Jg. (1977), pp. 272-278.

- /19/ S. C. Maclean, DT Fusion Neutron Irradiation of LASL-BNL Superconductor Wires, LLL Copper Tensile Specimens, ORNL Magnesium Oxide Crystal, UW-LLL High Purity Metallic Foils, and SLL Fiber Optic Bundles. UCID-16754 (1975).

- /20/ D. M. Parkin, D. G. Schweitzer, Stability of Multifilamentary Superconducting Magnet Materials to Neutron Irradiation. Trans. Amer. Nucl. Soc. 17 (1973) p. 147
- /21/ D. M. Parkin, A. R. Sweedler, Neutron Irradiation of Nb₃Sn and NbTi Multifilamentary Composites. LA-UR-74-1453, ASC, Oakbrook, 1974.
- /22/ T. Okada, Y. Hayashiuchi, Neutron Irradiation Effect on NbTi and Nb₃Sn and their Application in Superconducting Magnets for Fusion Reactors. J. of Nucl. Mat. 72 (1978), pp. 177-181.
- /23/ H. Tsubakihara et al., Neutron Irradiation Effects on Superconducting Materials in Thermonuclear Fusion Reactor Technology. 5th Int. Cryog. Conf., Kyoto, 1974.
- /24/ S. Takamura, T. Kato, Effect of Low Temperature Irradiation on Insulators and other Materials for Superconducting Magnets. J. of Nucl. Mat. 103 + 104 (1981), pp. 729-734.
- /25/ R. A. van Konynenburg et al., Fusion Neutron Damage in Superconductors and Magnet Stabilizers. J. of Nucl. Mat. 103 + 104 (1981), pp. 739-744.
- /26/ H. W. Weber et al., Neutron Irradiation of NbTi Superconductors. IEEE Trans. on Magn., Vol. MAG-17, No. 5, Sept. 1981, pp. 1711-1713.
- /27/ F. Nardai et al., Neutron Irradiation of a Broad Spectrum of NbTi Superconductors. Cryogenics 21 (1981), p 223.
- /28/ C. E. Oberly, The Effect of 14 MeV Neutron Heat Deposition on Nb₃Sn Superconducting Tubes. Air Force Aero-Propulsion Lab. Techn. Report AFAPL-TR-68-147, 1969.

- /29/ C. L. Snead jr. et al., Determination of the Damage-energy Cross Section of 14 MeV Neutrons from Critical-property Changes in Irradiated Nb₃Sn. BNL-21953, 1976.
- /30/ M. Soell et al., Influence of Disordering by Low-temperature Neutron Irradiation on the Superconducting Transition Temperature of Nb₃Sn. J. of Low Temp. Phys. Vol. 24, No. 5/6, 1976.
- /31/ S. L. Colucci et al., Critical Currents in Nb₃Sn Fast-neutron Irradiated at 6 K. Appl. Phys. Lett., Vol. 28, No. 11, 1976.
- /32/ B. S. Brown et al., Changes in the Superconducting Critical Temperature after Fast-neutron Irradiation. J. of Appl. Phys., Vol. 48, No. 4, 1977.
- /33/ C. S. Pande, A Mechanism for the Degradation of Superconducting Transition Temperature on High Energy Neutron Irradiation in A-15 Compounds. BNL-23053, 1977.
- /34/ S. L. Colucci et al., Critical Current Enhancement in Nb₃Sn by Low-temperature Fast-neutron Irradiation. J. of Appl. Phys., Vol. 48, No. 2, Febr. 1977.
- /35/ C. L. Snead jr., Changes in the Upper Critical Fields and Critical Currents of Nb₃Sn and V₃Ga Owing to Neutron Radiation Damage. Appl. Phys. Lett., Vol. 30, No. 12, 1977.
- /36/ B. S. Brown et al., J_C Changes after Neutron Irradiation of Nb₃Sn at 8 K. IEEE Transactions on Magnetics, Vol. MAG-13, No. 1, 1977.
- /37/ C. S. Pande, Nature of the Defects on Irradiated A-15 Compounds. BNL-24154, 15th Conf. on Low Temp. Phys., Grenoble, 1978.

- /38/ R. Viswanathan et al., Superconductivity in Irradiated A-15 Compounds at Low Fluences. I. Neutron Irradiated V_3Si . J. of Low Temp. Phys., Vol. 30, No. 3/4, 1978.
- /39/ B. S. Brown et al., Critical Current Changes in Neutron-irradiated Nb_3Sn as a Function of Irradiation Temperature and Initial Metallurgy. J. Appl. Phys. 49 (7), 1978.
- /40/ P. Maier, E. Seibt, Low-temperature Deuteron Irradiation of Differently Reacted Nb_3Sn Superconductors. J. of Nucl. Mat. 72 (1978), pp. 291-295.
- /41/ R. M. Scanlan, E. L. Raymond, Low Temperature Irradiations of Nb_3Sn with 14 MeV Neutrons. IEEE Trans. on Magn., Vol. MAG-15, No. 1, 1979.
- /42/ R. M. Scanlan, E. L. Raymond, Radiation Behaviour of Superconductors. In Special Purpose Materials. Annual Progress Report. DOE/ET-0095, 1979.
- /43/ C. L. Snead jr., M. Suenaga, Synergism between Strain and Neutron Irradiation in Filamentary Nb_3Sn Conductors. Appl. Phys. Lett. 37 (7), 1980.
- /44/ M. Fähnle, Radiation Effects on Superconductivity in A-15 Materials. IEEE Trans. on Mag., Vol. MAG-17, No. 5, 1981.
- /45/ C. L. Snead jr. et al., High Energy Neutron Damage in Nb_3Sn : Changes in Critical Properties and Damage Energy Analysis. J. of Nucl. Mat. 103 + 104 (1981), pp. 749-754.
- /46/ M.-H. Gely et al., Neutron Radiation Damage in Superconductor Nb_3Ge . J. of Nucl. Mat 103 + 104 (1981), pp. 745-748.
- /47/ P. Maier, E. Seibt, Volume Pinning Force and Upper Critical Field of Irradiated Nb_3Sn . Appl. Phys. Lett. 39 (2), 1981.

- /48/ J. E. Ostenson et al., Irradiation Effects for In-situ Composite Conductors. BNL-32384, ASC 1982, Knoxville.
- /49/ P. Müller et al., Ion and Neutron Damage Studies of A-15 Superconductors. J. of Nucl. Mat. 108 + 109 (1982), pp. 585-592.
- /50/ A. R. Sweedler et al., Neutron Irradiation of Superconducting Compounds. J. of Nucl. Mat. 72 (1978), pp. 50-69.
- /51/ D. Lambrecht, Status of Development of Superconducting AC Generators. IEEE Trans. on Magnetics, Vol. MAG-17,(5) 1981. pp. 1551-1559
- /52/ G. W. Cullen, R. L. Novak, J. Appl. Phys. 37 (1966), p. 3348.
- /53/ M. W. Thompson, Defects and Radiation Damage in Metals. Cambridge, University Press, 1969.
- /54/ B. S. Brown et al., Low-Temperature Fast-Neutron Radiation, Damage Studies in Superconducting Materials. J. of Nucl. Mat. 52 (1974), pp. 215-228.
- /55/ J. A. Horak, T. H. Blewitt, Fast- and Thermal-neutron Irradiation and Annealing of Cu, Ni, Fe, Ti and Pd. Nucl. Techn. Vol. 27, Nov. 1975, pp. 416-438.
- /56/ J. M. Williams et al., The Effects of Irradiation on the Copper Normal Metal of a Composite Superconductor. IEEE Trans. on Magn., Vol. MAG-15, No. 1, 1979.
- /57/ C. E. Klabunde et al., The Effects of Irradiation on the Normal Metal of a Composite Superconductor: A Comparison of Copper and Aluminum. J. of Nucl. Mat. 85 & 86 (1979), pp. 385-389.

- /58/ R. E. Nygren, Radiation Damage in the Copper Stabilizer in a Superconducting Magnet. J. of Nucl. Mat. 103 & 104 (1981), pp. 735-738.
- /59/ R. L. Chaplin, R. R. Coltman, jr., Defects and Transmutations in Reactor-Irradiated Copper. J. of Nucl. Mat. 108 & 109 (1982), pp. 175-182.
- /60/ M. W. Guinan, Radiation Effects Limits on Copper in Superconducting Magnets. May 1983, UCID-19800.
- /61/ R. R. Coltman, jr., Organic Insulators and the Copper Stabilizer for Fusion Reactor Magnets. J. of Nucl. Mat. 108 & 109 (1982), pp. 559-571.
- /62/ M. Nakagawa et al., High-dose neutron-irradiation effects in fcc metals at 4.7 K. Phys. Rev. B 16, 5285 (1977).
- /63/ T. H. Blewitt, Radiation Damage in Solids, ed. Billington, London, Academic Press, 1962.
- /64/ G. Burger et al., Analysis of Radiation Annealing Observed during Low Temperature Irradiation with Neutrons and Heavy Charged Particles. phys. stat. sol. 4, 281 (1964).
- /65/ J. A. Horak, T. H. Blewitt, Isochronal Recovery of Fast Neutron Irradiated Metals. J. of Nucl. Mat. 49 (1973/74), pp. 161-180.
- /66/ P. Jung et al., Defect Production Rates by Electrons, Ions and Neutrons in Cubic Metals. Proc. of the 11th Int. Symp. on Effects of Radiation on Materials. Brager/Perrin (eds.), ASTM Special Techn. Publ. 782, 1982, pp. 963-982
- /67/ R. R. Coltman et al., Reactor Damage in Pure Metals, J. of Appl. Phys., 33, 3509 (1962).

- /68/ R. R. Coltman et al., Survey of Thermal-neutron Damage in Pure Metals. Phys. Rev., 156 (1967) 715.
- /69/ K. Böning et al., The Kohler Rule of Magnetoresistance in Neutron-Irradiated Aluminum at 4.6 K. phys. stat. sol. 34, 395 (1969).
- /70/ K. Böning et al., Die Kohler-Regel für den longitudinalen Magnetowiderstand von neutronenbestrahltem Kupfer bei 4.6 K. Phys. Kondens. Materie 12, 72-80 (1970).
- /71/ J. A. Horak, T. H. Blewitt, Fast Neutron Irradiation Induced Resistivity in Metals. phys. stat. sol. (a) 9, 721 (1972).
- /72/ J. B. Roberto et al., Damage production by high-energy d-Be neutrons in Cu, Nb, and Pt at 4.2 K. Appl. Phys. Lett. 30, 509 (1977).
- /73/ R. R. Coltman jr. et al., Rates of Defect Production by Fission Neutrons in Metals at 4.7 K, J. of Nucl. Mat. 99 (1981), pp. 284-293.
- /74/ C. E. Klabunde, R. R. Coltman jr., Fission Neutron Damage Rates and Efficiencies in Several Metals. J. of Nucl. Mat. 108 & 109 (1982), pp. 183-193.
- /75/ G. Burger et al., Erholung des elektrischen Widerstandes reiner Metalle nach Neutronenbestrahlung bei 4,6 K im Reaktor. Z. Angew. Phys. 22, 452 (1967).
- /76/ K. Böning et al., Inelastic Neutron Scattering Measurements of Phonon Dispersion Curves in Reactor-Irradiated Aluminum at 4.6 K, Phys. Rev. Lett., 38, 852 (1977).
- /77/ M. W. Guinan, R. A. van Konynenburg, Fusion Neutron Effects on Magnetoresistivity of Copper Stabilizer Materials. UCRL-90134 (to be published in J. of Nucl. Mat.) 1983.

- /78/ P. Turowski et al., IEEE Trans. Magn., MAG-17 (1981), p. 2047.
- /79/ S. O. Hong et al., A Preliminary Design of the End Plug Magnet System for a Tandem Mirror Reactor. UWFDM-344, Proc. of the 8th Symp. on Eng. Probl. of Fusion Research, San Francisco, CA, 1979.
- /80/ R. L. Keizer, M. Mottier, Radiation-Resistant Magnets. CERN 82-05.
- /81/ J. H. Schultz, Design Practice and Operational Experience of Highly Irradiated, High Performance Normal Magnets. Journal of Fusion Energy, Vol. 3, No. 2, 1983, pp. 119-147.
- /82/ J. H. Schultz, A Costing and Sizing Code for Highly Irradiated Normal Magnets. MIT Research Report PFC/RR-81-13.
- /83/ B. J. Maddock, G. B. James, Protection and stabilisation of large superconducting coils. Proc. IEE, Vol. 115, No. 4 (1968), pp. 543-547.